Study on the Viscoelastic Properties of Cellulose in Dilute Ionic Liquid Solutions

徐, 哲

Study on the Viscoelastic Properties of Cellulose in Dilute Ionic Liquid Solutions

（セルロースイオン液体希薄溶液の粘弾性）

XU ZHE

徐　哲

Department of Molecular &Material Sciences

Interdisciplinary Graduate School of Engineering Sciences

Kyushu University

CONTENTS

Chapter 1 Introduction

1.1 Cellulose and Ionic Liquids

Along with the development of petrochemical industry and increasing of world population, the consumption demands for synthetic polymer goods replacing traditional ones have increased significantly, especially in developing countries. The synthetic polymers are relying on the use of depleting fossilized organic matter. The fossil feedstock is limited on the earth. The awareness of sustainable resource has raised the interest in renewable resources and environmental-friendly processes. Cellulose which is the most abundant natural polymer in the world offers new opportunities in the development of alternative raw material for chemicals and fuels.

Cellulose was discovered by A. Payen who isolated it from plant and determined its chemical formula in 1838.[1)-3)] As we all know that the plants are mainly composed of cellulose. For example, cellulose content is 40-50% of wood, 57% of dried hemp and the cotton is almost the pure cellulose.

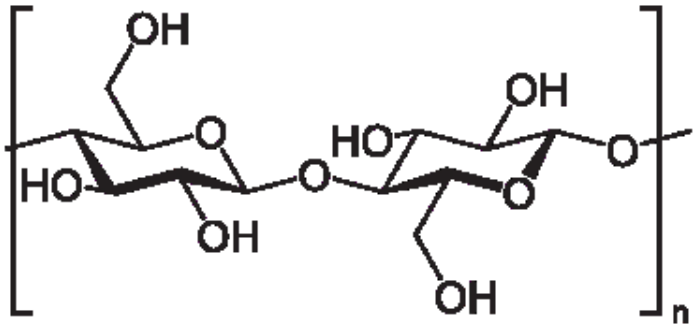

Figure 1-1. Molecular structure of cellulose.

Cellulose is made up of D-glucose units, which condense through β (1→4)-glycosidic bonds. It is believed to be a linear polymer chain. As shown in Figure 1, there exists a large numbers of –OH groups in cellulose molecular chain. The intramolecular and intermolecular hydrogen bonds are formed by the –OH groups. It is known that cellulose cannot achieve molten state or to be uniformly dissolved in water and conventional organic solvents due to the intra- and intermolecular hydrogen bonds, which makes cellulose processing a challenging task.[4), 5)] until now, more than 100 solvent systems for cellulose have been reported.[6)] The typical cellulose solvents are such as N,N-dimethylacetamide/lithium chloride (DMAc/LiCl)[7)-9)], N-methylmorpholine oxide (NMMO)[10)], tetrabutylammonium fluorides/dimethyl sulfoxide mixture (TBAF/DMSO)[11)], N,N-dimethylformamide/nitrous tetroxide (DMF/N_2O_4)[12)], dimethyl sulfoxide (DMSO)/ammonium fluorides[13), 14)], and molten salt hydrates, for example, $LiClO_4 \cdot 3H_2O$ and $LiSCN \cdot 2H_2O$[15)].

Among these solvents, the NMMO is the only one used in industry to manufacture cellulose fibers, and the process is called Lyocell process. However, there are still some drawbacks for Lyocell process. The thermal instability of NMMO demands higher safety technology to keep NMMO stable and to prevent cellulose from degradation. Before the Lyocell process, the viscose process was wildly used to manufacture cellulose fibers in 1990s. The viscose process was carried out as the following steps: (1) the cellulose was treated with aqueous sodium hydroxide to form alkali cellulose; (2) the alkali cellulose was treated with carbon disulfide to form the highly viscous sodium cellulose xanthate solution; (3) after depolymerization the

solution was washed with acids to regenerate the cellulose. The viscose process caused serious energy and environmental problems. Therefore, it is necessary to develop a new kind of "green" cellulose process method and suitable dissolution approaches to make further cultivation of cellulose resources.

Ionic liquid is a generic name for a group of organic salts that exist in liquid state at relatively low temperatures, usually<100 °C, due to their poorly coordinated cations and anions[16), 17)]. Because of their attractive properties, such as chemical and thermal stability, low vapor pressure, low melting point, high ionic conductivity, compared to the traditional violate organic solvent, they are "green" and widely used in sciences and engineering fields including catalysts[18)], synthesis[18), 19)], physical chemistry[20), 21)], and advanced materials. [22)- 24)]

Graenacher discovered the molten pyridine-N-oxide chloride salts, could dissolve the cellulose in 1934.[25)] This might be the first example of cellulose being dissolved with ionic liquids (ILs). However, because of the high melting point the concept of ILs had not been pushed forward at that time. The development of ILs stopped for a few decades. After the pioneering work of Swatloski *et al*[26)], many kind of ILs are found to be the solvent for cellulose. Consequently, a number of studies for cellulose dissolved in ILs have rapidly increased in the past decade, as accumulated in a several recent reviews.[27)-33)] The mechanism of cellulose dissolution in ILs is generally accepted that the native hydrogen-bonded network in cellulose is destroyed by the new hydrogen bonds formed by anions of ILs with the hydroxyl groups of cellulose. The most frequently used ILs as the solvent for cellulose are

1-butyl-3-methylimidazolium chloride (BmimCl)[26], 1-allyl-3-methylimidazolium chloride (AmimCl)[34] and 1-ethyl-3-methylimidazolium acetate (EmimAc)[35].

It is necessary to study solution properties of polymer/ILs to obtain the information on the structure of polymers in ILs solutions to further develop the commercial use. However, conventional characterization methods are difficult to apply to IL solutions. Therefore, the solution structure of cellulose has been mainly characterized by rheological measurements. Rheological studies of cellulose solutions in ILs can be linked to the molecular conformation of cellulose through the knowledge of dilute solution properties of polymers, it also be a major linking with the molecular characteristics and applications.[36] As a result, rheological measurements are used to characterize the solutions in the most of studies and sometimes degradation of cellulose was pointed out from the change in the rheological data.[37)-46)]

Haward *et al*[47)-49)] briefly summarized that the degradation of cellulose become significant for chloride-based ILs heated above, say 100 °C but the degradation is not so severe when EmimAc is used at lower temperature. The majority of studies aimed at commercial use of the IL solutions for processing and derivatization of cellulose so that cellulose samples from different origin and different dissolution methods are tested. Therefore, it is very difficult to compare the results so far published from the point view of degradation. A few recent studies attempt to examine effects of dissolution methods but there remains many conditions which is not examined.

Although the degradation of cellulose in the dissolution process and solution storage is a big problem for the further processing, it also may mean that there is a

possibility to control the molecular weight of cellulose by dissolving into ILs at different conditions. To investigate the rheological properties of cellulose in ILs, it is essential to utilize the knowledge of dilute solution properties of polymers, which is briefly summarized in the following subsections.

1.2 Physical properties of polymers in dilute solution

The flexible polymers in solvents can be classified into three regions. The critical concentration at which polymer coils begin to overlap with each other is called overlapping concentration (C^*).[50)-53)] It is defined as:

$$C^*=3M/(4\pi N_A R_g^3) \quad (1)$$

Where N_A is the Avogadro's number, M is the polymer molecular weight, R_g is the radius of gyration of polymer chain. The solvent power (thermodynamic factor) is incorporated with R_g. When the concentration of polymer solution (C) fulfills $C < C^*$, the polymer chains are separated from each other and behave more or less independently. The chains primarily interact with the solvent. At this state, the solution is close to an ideal solution. As C increases, the interactions among the chains get stronger, at $C = C^*$, the chains begin to overlap with each other. When $C > C^*$, the solution is called semi-dilute, the chains are overlapped and/or entangled. Compared with the solution in dilute region, the mobility of the chains reduce greatly though the interaction is the thermodynamic properties are almost the same as in the dilute region but partially screened. When C exceeds 0.2~0.3g/cm^3, the solution enters into

concentrated region in which each segment of the polymer chain does not have a sufficient space available and the thermodynamic interactions are shielded by dense segment.

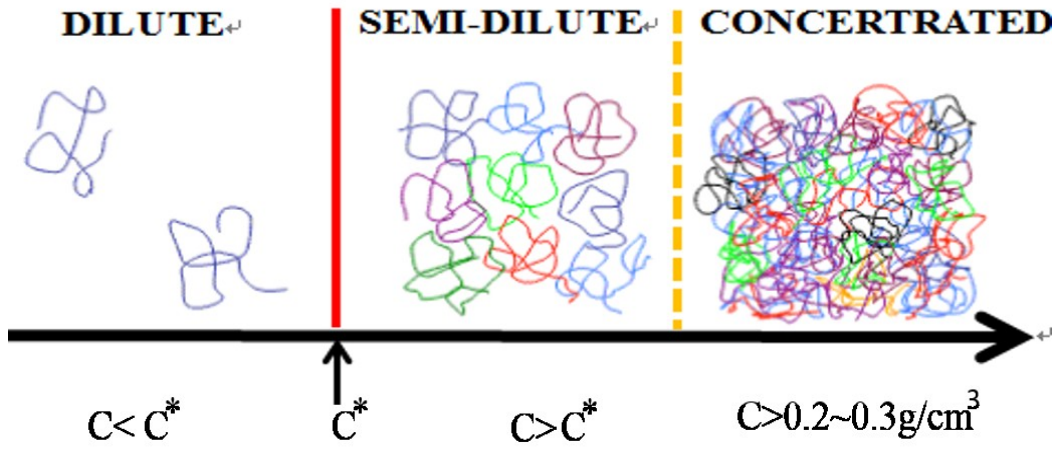

Figure 1-2. Concertration regimes for linear flexible polymer solutions

To understand the behavior of single polymer chain, it is needed to study in the dilute region and many experimental methods are established. Among them, most primitive but most useful one intrinsic viscosity [η] measurement which express hydrodynamic size of the polymer coil.[54] It can be obtained from measurements of the pure solvent viscosity η_s and zero-shear viscosity η^0 of solutions. The relative viscosity $\eta_{rel}=\eta^0/\eta_s$ and specific viscosity $\eta_{sp}=\eta_{rel}$-1 are usually used to obtain [η], it can be obtained by the extrapolated the plots of η_{sp}/C and $\ln\eta_{rel}/C$ vs C to the zero concentration limit.[55]

The Mark-Houwink-Sakurada (MHS) equation express the relationship between the

$[\eta]$ and the molecular weight M as equation 2.

$$[\eta]=KM^{\alpha} \qquad (2)$$

Where α=0.5 corresponds to Θ condition, α=0.7~0.8 corresponds to a good solvent condition for most of linear flexible polymers.

Corresponding statistical size of polymer chain is given by R_g, related to M as $R_g \propto M^{\upsilon}$. For Gaussian chain in Θ solvent υ=0.5 , while υ=0.6 corresponds to the expanded size in good solvents.[56] $[\eta]$ can be related with R_g and M by employing the Flory-Fox viscosity equation as

$$[\eta]=\phi(R_g^2)^{3/2}/M \qquad (3)$$

Where ϕ is the Flory viscosity factor. In this case, the relationship between $[\eta]$ and M can be expressed as $[\eta] \propto M^{\alpha} \propto M^{3\upsilon-1}$. Then by employing the equation 1, the relationship between C^* and $[\eta]$ can be expressed as $C^* \simeq 1/[\eta]$. For the flexible polymer solutions, the reported equations can be used to estimate M. When molecular weight distribution (MWD) is narrow, M obtained from the equation.2 is closed to the weight-average molecular weight M_w.

The viscoelastic properties of flexible polymers in dilute solution can be discussed with the bead-spring model as started by Rouse and Zimm. As illustrated in Figure 1-3, this model is composed by N+1 beads which represent the frictional elements connected with N springs. The springs are represented as the statistical segments. As described by Rouse theory, there are no hydrodynamic interactions between the beads, the polymer chains are the free draining Gaussian chains.[57] An important extension was made by Zimm, the strong hydrodynamic interactions among beads was

employed in Zimm theory.[58)]

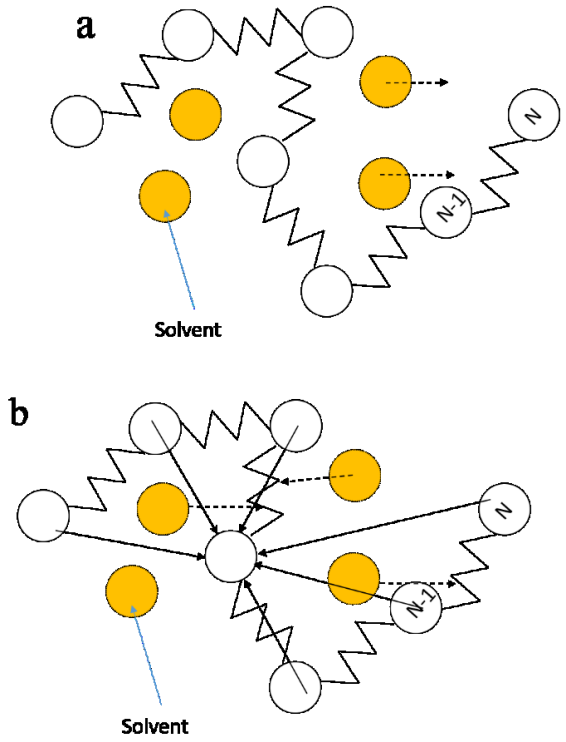

Figure 1-3. Bead-spring model of Rouse (a) and Zimm (b) theory

As a sum, viscoelastic properties of linear flexible polymers in dilute solution can be expressed by general formulas of Rouse-Zimm (RZ) model. For dynamic viscoelasticity, storage modulus *G*' and the loss modulus *G*", can be expressed by the following general formulae,

$$G''(\omega) = \frac{CRT}{M} \sum_{p=1}^{N} \frac{\omega \ \tau_P}{1+\omega^2 {\tau_P}^2} + G''(solvent) \qquad (4)$$

$$G'(\omega) = \frac{CRT}{M} \sum_{p=1}^{N} \frac{\omega^2 {\tau_P}^2}{1+\omega^2 {\tau_P}^2} \qquad (5)$$

$$G''(solvent) = \omega\eta_s \tag{6}$$

$$\tau_p = \frac{\tau_{RZ}}{p^{\alpha}} \tag{7}$$

Where C is the polymer concentration, R is the gas constant, T is the absolute temperature, M is the molecular weight, ω is the frequency and η_s is solvent viscosity. τ_p is the relaxation time of p-th normal mode defined in eq.7 where τ_{RZ} is the longest relaxation time, which can be phenomenologically obtained from the terminal region data. The parameter α denotes the hydrodynamic interaction strength; α = 2 corresponds to non-draining limit, while α = 1.5 corresponds to free-draining limit.[57] Another definition for the longest relaxation time is given in Rouse model, when the η_s is small enough to be neglected

$$\tau_p = \frac{6\eta^0 M}{\pi^2 p^2 CRT} \tag{8}$$

Where τ_p is p-th relaxation time in the Rouse model and τ_1 is the longest one.

The original RZ theories argue Gaussian chains at infinite dilute region. However, the Rouse model can explain the linear viscoelastic properties of non-entangled melts very well over a wide range of ω.[58), 59)] It should be noted that when measuring temperature is not far from the glass transition temperature T_g[58)], the contributions from glassy zone G^*_G cannot be neglected in dynamic moduli G^*. This is also true for the solutions in which glass forming solvents are used.[60)] It is known that for non-entangled solutions with the increase of C, the behavior of G^* change from Zimm-like to Rouse-like.

Osaki *et al.*[61] systematically studied G^* data for standard polystyrene in a good solvent and introduced correction term to get a good fitting result at low ω region which was called long-time (LT) term;

$$G'_{LT} = G_{LT} \frac{\tau_{LT}{}^2 \omega^2}{1+\tau_{LT}{}^2 \omega^2} \tag{9}$$

$$G''_{LT} = G_{LT} \frac{\tau_{LT} \omega}{1+\tau_{LT}{}^2 \omega^2} \tag{10}$$

$$G_{LT} = QC[\eta]\frac{CRT}{M} \tag{11}$$

$$\tau_{LT} = P\tau_{RZ} \tag{12}$$

where Q and P being adjustable parameters (Q = 0.09 and P = 5 in their study). The calculated G" of LT term is almost the same as the original RZ fitting, while G' data in the lower frequency region can be well fitted by addition of the LT term.

The hydrodynamic radius of polymer chain at infinite dilution is linked with LT term by intrinsic viscosity $[\eta]$. With the increasing of C, the changes in hydrodynamic interaction can be expressed by the coil overlapping degree $C/C^* \sim C[\eta]$. In their study, chain overlapping concentration C^* is set as $C^* = 2.5/[\eta]$ according to the Einstein's viscosity equation[62]. Note that the results for thermodynamic properties such as osmotic pressure and correlation length[52] have good agreement with the transition from dilute to semi-dilute region obtained by viscoelastic properties.

1.3 Research Objectives

The first object of this research is examination of dissolution methods of cellulose from different origins into imidazolium based ILs to establish the ways to get uniform

solutions without severe degradation of cellulose molecules. The M_w will be estimated from the dynamic viscoelastic properties to check how M_w changed under different dissolving conditions. For that purpose, we examine applicability of Rouse-Zimm model to the viscoelastic properties and propose a molecular estimation method. By such studies, we aim to clarify the molecular characteristics of cellulose which will be important to develop new commodity plastic and elastomeric materials from natural resources without chemical reactions to preserve bio-degradation ability.

The following part of this thesis is structured as follows: The general experimental methods are summarized in chapter 2. In chapter 3, dissolution conditions of cellulose from different origins into BmimCl, AmimCl and EmimAc are examined. In chapter 4, the viscoelastic properties of cellulose in ILs are studied by using Rouse-Zimm mode. An application for determining the M_w by using Rouse-Zimm model fitting is discussed in this section. In chapter 5, the influence of water content in both cellulose and ILs on M_w for dissolved cellulose are discussed. Chapter 6 is the conclusion of this thesis.

1.4 Reference

1) Liang CY and Marchessault RH, *J. Polym. Sci*. **39**, 269 (1959).

2) Blackwell J, Kolpak FJ and Gardner KH, *ACS Symp. Ser*. **48**, 42 (1977).

3) Crawford RL, *Lignin biodegradation and transformation* John Wiley and Sons, New York (1981).

4) Pinkert A, Marsh KN, Pang S and Staiger MP, *Chem. Rev.*, **109**, 6712–6728 (2009).

5) Wang H, Gurau G and Rogers RD, *Chem. Soc. Rev*. **41**, 1519–1537(2012).

6) Cellolose Gakkai, "*Cellulose no Jiten*", Asakura Shoten, Tokyo (2000).

7) McCormick CL, Callais PA, Hutchinson BH, *Macromolecules,* **18**, 2394–2401 (1985).

8) McCormick CL and Dawsey TR, *Macromolecules*, **23**, 3606−3610 (1990).

9) Matsumoto T, Tatsumi D, Tamai N, Takaki T, *Cellulose,* **8**, 275–282 (2001).

10) Fink HP, Weigel P, Purz HJ, Ganster J, *Prog. Polym. Sci.* **26**, 1473–1524 (2001).

11) Heinze T, Dicke R, Koschella A, Kull, AH, Klohr, EA, Koch W *Macromol. Chem. Phys*., *201*, 627– 631 (2000).

12) Hammer RB and Turbak AF., *Abstracts of Papers of the American Chemical Society*, **173**, 8−8 (1977).

13) Ciacco GT, Liebert TF, Frollini E,and Heinze TJ, *Cellulose*, **10**, 125−132 (2003).

14) Ramos LA, Frollini E, Heinze T, *Carbohydr. Polym.,* **60**, 259–267 (2005).

15) Fischer S, Leipner H, Thu¨mmler K, Brendler B, Peters J, *Cellulose* **10**, 227–236 (2003).

16) Ohno H, *"Ionic liquids: The Front and Future of Material Development"*, **CMC** Shuppan, Tokyo (2006).

17) Rogers RD and Seddon KR, *Science*, **302**, 792−793 (2003).

18) Welton T. *Chem. Rev.*, **99**, 2071-2083, (1999).

19) Kubisa, P. *J. Polym. Sci. Part A: Polym. Chem.* **43**, 4675–4683 (2005).

20) Seddon KR, Stark A; Torres MJ, *Pure. Appl. Chem.*, **72**, 2275-2287 (2000).

21) Yang QW; Zhang H, Su BG, Yang YW, Ren QL and Xing HB, *J. Chem. Eng.*

55, 1750–1754 (2010).

22) Poplin JH, Swatloski RP, Holbrey JD, Spear SK, Metlen A, Gratzel M, Nazeeruddin MK, Rogers RD *ChemCommun* (UK). **20**, 2025 (2007).

23) Wu J, Zhang J, Zhang H, He J, Ren Q, Guo M, *Biomacromolecules.* **5**, 266–268 (2005).

24) Lu J, Yan F, Texter J, *Prog. Polym. Sci.* **34**, 431 (2009).

25) Graenacher C, *US Pat*, 1943176, 1934.

26) Swatloski RP, Spear SK, John D, Holbrey JD and Rogers RD, *J. Am. Chem.* Soc., 2002, **124**, 4974–4975.

27) Zhu S, Wu Y, Chen Q, Yu Z, Wang C, Jin S, Ding Y, Wu G, *Green Chem*, **8**, 325–327 (2006).

28) Pinkert A, Marsh KN, Pang S and Staiger MP, *Chem. Rev*, **109**, 6712–6728 (2009).

29) Wang H, Gurau G, Rogers RD, *Chem. Soc. Rev*, 41, 1519– 1537 (2012).

30) Brandt A, Grasvik J, Hallett JP and Welton T, *Green Chem*, 15, 550–583S (2013).

31) Badgujar KC and Bhanage BM, *Bioresour. Technol*, **178**, 2–18 (2015).

32) Hina S, Zhang Y, Wang H, *Rev. Adv. Mater. Sci*, **40**, 215-226 (2015).

33) Kang XY, Kugaa S, Wang L, Wu M, Huang Y. *Journal of Bioresources and Bioproducts*, **1**,(2) (2016).

34) Zhang H, Wu J, Zhang J and He SJ, *Macromolecules*, **38**, 8272–8277 (2005).

35) Kosan B, Michels C, Meister F, *Cellulose*, **15**, 59-66 (2008).

36) Ferry JD, "*Viscoelastic Properties of Polymers*", 3rd ed, , John Wile & Sons Inc, NY (1980).

37) Kuang QL, Zhao JC, Niu YH, Zhang J and Wang ZG, *J. Phys. Chem. B*, **112**,

10234–10240 (2008).

38) Gericke M, Schlufter K, Liebert T, Heinze T and Budtova T, *Biomacromolecules*, **10**, 1188–1194 (2009).

39) Collier JR, Watson JL, Collier BJ, and Petrovan S, *J. Appl. Polym. Sci*, **111**, 1019–1027 (2009).

40) Chen X, Zhang Y, Cheng L and Wang H, *J. Polym. Environ*, **17**, 273–279 (2009).

41) Sescousse R, Le KA, Ries ME and Budtova T, *J. Phys. Chem. B*, **114**, 7222–7228 (2010).

42) Chen X, Zhang Y, Wang H, Wang SW, Liang S and Colby RH, *J. Rheol*., **55**, 485–494 (2011).

43) Song H, Niu Y, Wang Z and Zhang J, *Biomacromolecules*, **12**, 1087–1096 (2011).

44) Lu F, Cheng B, Song J and Liang Y, *J. Appl. Polym. Sci.*, **124**, 3419–3425 (2012).

45) Haward SJ, Sharma V, Butts CP, McKinley GH and Rahatekar SS, *Biomacromolecules*, **13**, 1688–1699 (2012).

46) Lu F, Song J, Cheng BW, Ji XJ and Wang LJ, *Cellulose*, **20**, 1343–1352 (2013).

47) Michud A, Hummel M, Haward S and Sixta H, *Carbohydr. Polym*., **117**, 355–363 (2015).

48) Karatzos S, Edye L and Wellard R, *Cellulose*, **19**, 307–312 (2012).

49) Clough MT, Geyer K, Hunt PA, Son S, Vagt U and Welton T, *Green Chem*, **17**, 231–243 (2015).

50) Noda I, Kato N, Kitano T, Nagasawa M, *Macromolecules*, **14**, 668 (1981).

51) Higo Y, Ueno N, Noda I, *Polym. J*., **15**, 367 (1983).

52) Noda I, Higo Y, Ueno N, Fujimoto T, *Macromolecules*, **17**, 1055 (1984).

53) Ying QC, Chu B, *Macromolecules*, **20**, 362-366 (1987).

54) Lapasin R, Pricl S, "*Rheology of industrial polysaccharides: theory and applications"* Blackie Academic and Professional, Glasgow (1995).

55) Huggins ML, *J. AM. Chem. Soc*, **64**, 2716–2718, (1942).

56) Doi M, Edwards SF, "*The Theory of Polymer Dynamics"* Oxford University Press, Oxford. (1986).

57) Rouse PE, *J Chem Phys,* **21**, 1272 (1953).

58) Zimm BH, *J Chem Phys,* **24**, 269 (1956).

59) Ferry JD, Landel RF, Williams ML, *Journal of Applied Physics,* **26**, 359 (1955).

60) Onogi S, Masuda T, Kitagawa K, *Macromolecules*, **3**, 109-116, (1970).

61) Osaki K, Inoue T, Uematsu T, *Journal of Polymer Science: Part B: Polymer Physics,* **39**, 211–217 (2001).

62) Osaki K, Inoue T, Uematsu T, Yamashita Y, *Journa of Polymer Science: Part B: Polymer Physics,* **40**, 1038–1045 (2002).

Chapter 2 Experiments & Fundamental data

2.1 Introduction

In this chapter, general experimental procedures for cellulose/IL systems used in this study are summarized. Further details for studies in each chapter are specified at corresponding part. The protocols used in this study are introduced to avoid moisture adsorption. However, we still need to examine the effect of water content on density and viscosity of the solutions.

Compared to conventional solvents[1)-2)], ILs are glass forming liquids so that the density and viscosity may have steep temperature dependence which more or less affected by moisture adsorption. In addition the densities of polysaccharides are normally higher than synthetic polymers.[3)] Therefore, the density of polymer/IL solutions cannot be assumed to be 1g/cm^3, as is done in the recent studies for polymer solutions. In order to make more precise discussion, it is essential to establish the empirical relationship between the concentration in *wt*% and in g/cm^3 [4)]. It is also needed to know temperature dependence of solvent viscosity in relation with water content. In this chapter, the densities of cellulose/ILs solutions up to 2.5*wt*% including the effects of remaining water[5)-7)] in ILs with the moisture adsorption of ILs will be examined. Solvent viscosity of ILs are also tabulated here.

2.2 Materials

BmimCl and AmimCl are synthesized and purified with activated carbon in our lab following the method in literatures with slight modification. [8)-10)] The synthesized ILs are crystallized and stocked in a refrigerator. The crystalline ILs are heated to be liquids and then gradually cooled to room temperature in the air. By the adsorption of moisture, these ILs became liquid even at the room temperature. EmimAc (nominal purity: 97%) was purchased from Aldrich, stocked in a refrigerator and used without further purification. ILs are dried in *vacuo* at 60 °C for 12 hours. The water content of ILs measured by Karl-Fischer titration (KEM, MKC-501) ranged in 1~1.5 *wt*% after the drying process.

Four kinds of cellulose are used in this research: avicel purchased from Merck, cosmetic cotton purchased from Cotton Lab, nadelholz sulfur pulp (NSP) sheet supplied from Daicel Corporation and linter pulp supplied from Shin-Etsu Chemical Co., Ltd.. The cotton and the NSP were tore into small pieces before being used. The drying experiment of cotton is carried out to find the suitable experiment condition for all the celluloses. The weight of cosmetic cotton samples (Cotton Lab), kept in a desiccator, become almost constant after dried in *vacuo* at 60 °C for 12 hours or longer drying time. The usual weight loss was about 6 – 7 %. To examine moisture adsorption, the dried sample was kept in ordinary room (about 25°C, 80% humidity) for 4 days, then the sample was dried again. Though the weight loss of samples kept in humid air is large (12 – 14 %), the difference of the weight of 3 samples after the first and second drying process are only about 1 %. Therefore, we can assume that the

free water adsorbed to cellulose can be removed by this drying process. We further dried the sample in *vacuo* at 110 °C and checked the additional weight loss, which was only about 3 – 4 % and very rapidly adsorb moisture to the level of after 60 °C drying process, confirming that the bonded water cannot be easily removed by drying. Therefore, the suitable drying process for all the celluloses is set at 60 °C for 12 hours.

2.3 Sample Preparation

Prescribed amounts of the cellulose samples and ILs are weighed and mixed into vial bottles or flasks under N_2 atmosphere in a nitrogen box to prepare solutions. Then the mixtures are degassed and purged with N_2 gas for few times in a vacuum oven to remove the oxygen before dissolution. To choose adequate temperature for uniform dissolution in appearance in a reasonable time span, first dissolution test was carried out for cotton/BmimCl under *vacuo* by directly connecting the flasks to vacuum pump and heating by oil bath. Effect of mechanical stirring was also tested. In this experiment, very violent bubble burst, which may cause chain cessation occurred. Therefore, the dissolution temperature for cotton/AmimCl and cotton/EmimAc are tested at 0.1 atm using vacuum oven connected to diaphragm pump.

At the selected temperatures, we further examined dissolution conditions for cellulose into ILs under N_2 gas atmosphere and 0.1 atm to obtain less colored uniform solution. At the beginning of the dissolution, bubble burst always observed for all the samples but it almost stopped when the sample mixtures became transparent. To observe the appearance of the solutions (macroscopic observation), vacuum oven was occasionally cooled to room temperature and purged by N_2 gas. Then heating in

vacuum oven was continued until the solutions became macroscopically uniform.

By the above experiments, we obtained a certain range of temperature, pressure and heating time appropriate for dissolution of cellulose with less degradation The chosen conditions will be mentioned in each section.

2.4 Density Measurements.

The density ρ (g/cm^3) of the cotton/BmimCl, cotton/AmimCl and cotton/EmimAc solutions for different concentrations were measured at atmospheric pressure in a DMA 4500 density meter (Anton paarGmbH) at different temperatures ranging from 10.00 °C to 80.00 °C. Temperature were controlled within ± 0.05 °C at each measurement. The uncertainty of the measurements was estimated to be better than ± 1×10^{-4} g/cm^{-3}.

2.5 Dynamic Viscoelastic Measurements.

Dynamic viscoelastic measurements of cellulose solutions are carried out in an MCR-300 rheometer (Anton Paar GmbH) equipped with peltier temperature control system with 50 mm diameter and 1 ° cone angle geometry under N_2 atmosphere at 40, 25, or 10 °C to cover the terminal region. The strain amplitude was kept small (< 0.1) to ensure the linearity of the data. As in the previous studies for pullulan/IL solutions[11), 12)], a homemade plastic chamber surrounding original chamber of instruments, purged by N_2 gas, was used and the measurement time was kept shorter than 30 min to prevent moisture adsorption during sample loading and the measurements.

2.6 Macro and Microscopic Observations of Dissolution Process

The samples for microscopic observation (ca. 3 mg each, 3 to 5 samples per a solution) were prepared and collected on a slide glass and shielded by a cover glass by the same manner as the macroscopic observation. Microscopic observation was carried out by a Keyence VHX-5900 digital microscope combined with VHX-S550 XYZ motorized free-angle observation system using VHX-ZST zoom lens (magnification: 20x to 2000x). High Dynamic Range function in transmission mode was used.

2.7 Fundamental data

2.7.1 Density

The values of density ρ for the cellulose/ILs solutions are listed in Table 1~3, Figure 2-1 and Figure 2-2, shows the *wt*% concentration *c* and the temperature *T* dependences of ρ for cellulose/ILs respectively, it is found in all the solutions that ρ increase linearly with the increase of *c* and decrease of *T*. Note that the density of pure AmimCl is obviously lower than the cellulose/AmimCl solution. From these results an empirical relationship of density and concentration can be obtained as

$$\rho = ac + \rho_0 \quad (g/cm^3) \qquad (1)$$

where ρ_0 is the density of pure IL. For the cellulose/ILs solutions, the results of *a* are summarized in Table 2-1~2-3. The uncertainty of *a* was estimated to be $\pm 2 \times 10^{-4}$

for cellulose/BmimCl solution, ±7 × 10^{-5} for cellulose/EmimAc solution and ±4 × 10^{-4} for cellulose/AmimCl solution. By calculating from the equation 1, the density of the cellulose/ILs solutions in any concentration in this range can be determined. Furthermore, the concentration C in g/cm^3 can be derived as

$$C = \rho c/100 \ (g/cm^3) \qquad (2)$$

It is complicated to discuss it near the glass transition temperature for the temperature dependence of density. However, at the T range from 10.00 °C to 80.00 °C, we obtained

$$\rho = bT + K \quad (g/cm^3) \qquad (3)$$

Where K is the value of density at 0 °C and the value of b for several concentrations are listed in Table 2-4&2-5. The uncertainty of b was estimated to be ± 5 × 10^{-6} for all solutions.

Table 2-1. Density ρ of cellulose/BmimCl solution from T = 10 °C to T = 80 °C

	ρ (g/cm^3)								
c (*wt*%)	10.00 °C	25.00 °C	30.00 °C	35.00 °C	40.00 °C	50.00 °C	60.00 °C	70.00 °C	80.00 °C
0.00	1.092	1.0834	1.0805	1.0775	1.0745	1.0685	1.0629	1.0574	1.0519
0.25	1.0929	1.0842	1.0813	1.0784	1.0754	1.0693	1.0638	1.0582	1.0527
0.49	1.0933	1.0847	1.0818	1.0789	1.0759	1.0698	1.0642	1.0587	1.0532
1	1.0948	1.0861	1.0833	1.0804	1.0774	1.0713	1.0657	1.0602	1.0547
1.49	1.0971	1.0885	1.0856	1.0827	1.0798	1.0736	1.0681	1.0626	1.0571
1.96	1.0983	1.0897	1.0868	1.084	1.0811	1.075	1.0693	1.0638	1.0583

Table 2-2. Density ρ of cellulose/AmimCl solution from T = 10 °C to T = 80 °C

	ρ (g/cm^3)								
c (*wt*%)	10.00 °C	25.00 °C	30.00 °C	35.00 °C	40.00 °C	50.00 °C	60.00 °C	70.00 °C	80.00 °C
0.00	1.1522	1.1425	1.1396	1.1366	1.1339	1.1279	1.1222	1.1166	1.1111
0.25	1.1567	1.1474	1.1441	1.1412	1.1383	1.1326	1.1268	1.1212	1.1157
0.5	1.1573	1.1481	1.1448	1.1419	1.139	1.1332	1.1275	1.1218	1.1162
1	1.1592	1.1501	1.1469	1.1438	1.1409	1.1352	1.1295	1.1239	1.1182
1.49	1.1612	1.1522	1.149	1.1458	1.1429	1.1372	1.1315	1.1259	1.1203
2.01	1.1631	1.1541	1.151	1.1477	1.1447	1.139	1.1333	1.1277	1.1221
2.47	1.1651	1.1562	1.1531	1.15	1.1467	1.141	1.1353	1.1297	1.1241

Table 2-3. Density ρ of cellulose/EmimAc solution from T = 10 °C to T = 80 °C

	ρ (g/cm^3)								
c (*wt*%)	10.00 °C	25.00 °C	30.00 °C	35.00 °C	40.00 °C	50.00 °C	60.00 °C	70.00 °C	80.00 °C
0.00	1.1084	1.099	1.096	1.0929	1.0899	1.0839	1.0779	1.07192	1.066
0.25	1.1095	1.1001	1.097	1.094	1.091	1.0849	1.0789	1.073	1.0671
0.5	1.1102	1.1008	1.0977	1.0946	1.0916	1.0856	1.0795	1.0736	1.0677
1	1.1122	1.1029	1.0998	1.0968	1.0937	1.0876	1.0816	1.0756	1.0696
1.51	1.1139	1.1046	1.1016	1.0985	1.0955	1.0894	1.0834	1.0775	1.0715
2.04	1.1155	1.1062	1.1032	1.1001	1.0971	1.091	1.085	1.0791	1.0732
2.47	1.1172	1.1079	1.1048	1.1018	1.0987	1.0927	1.0867	1.0807	1.0748

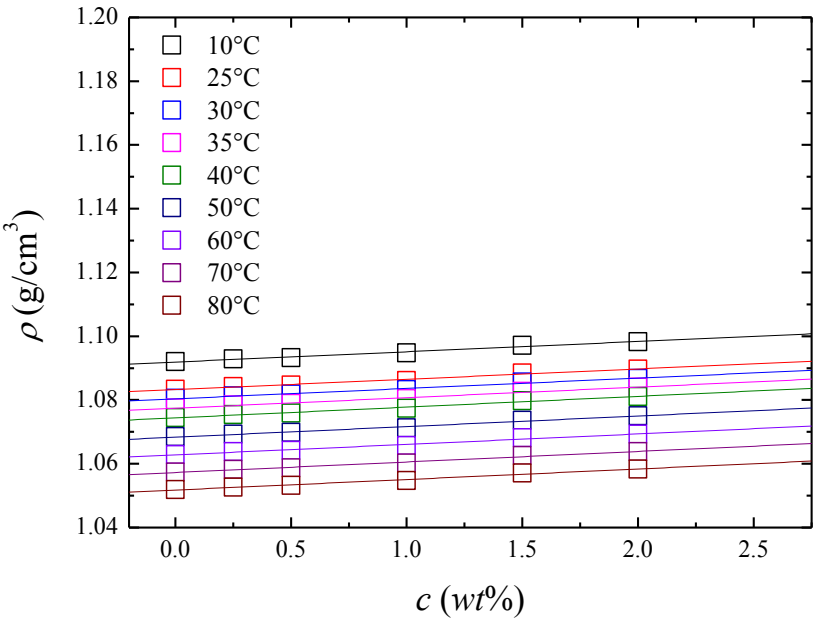

Figure 2-1-a. Concentration dependence of the density for cellulose/BmimCl solution at different temperatures.

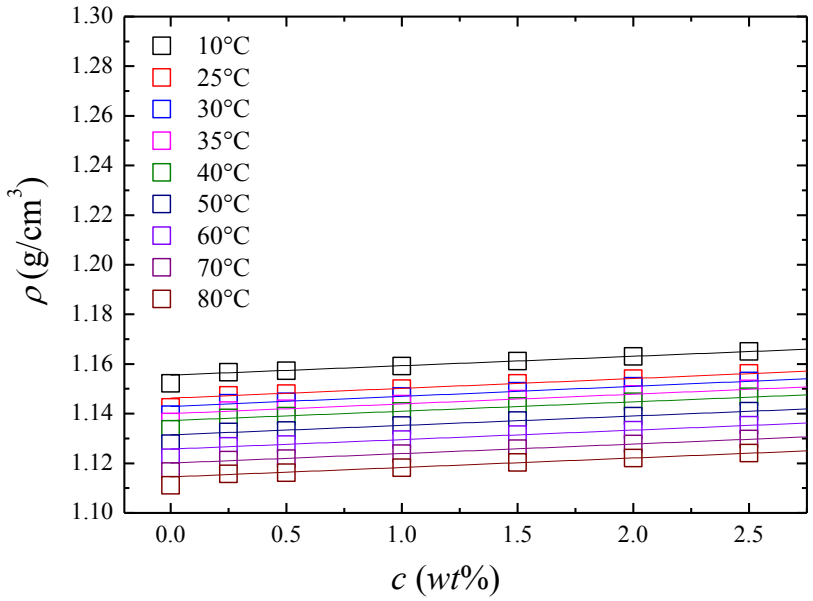

Figure 2-1-b. Concentration dependence of the density for cellulose/AmimCl solution at different temperatures.

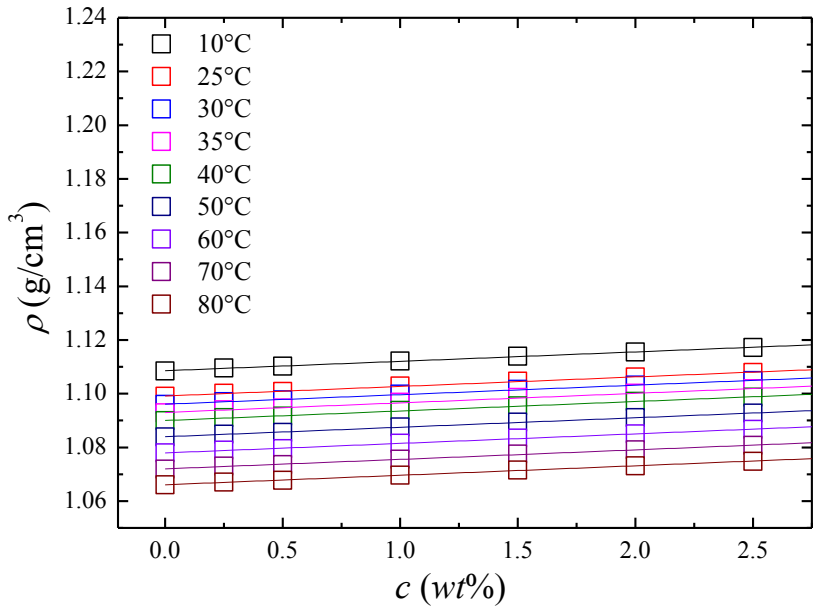

Figure 2-1-c. Concentration dependence of the density for cellulose/EmimAc solution at different temperatures.

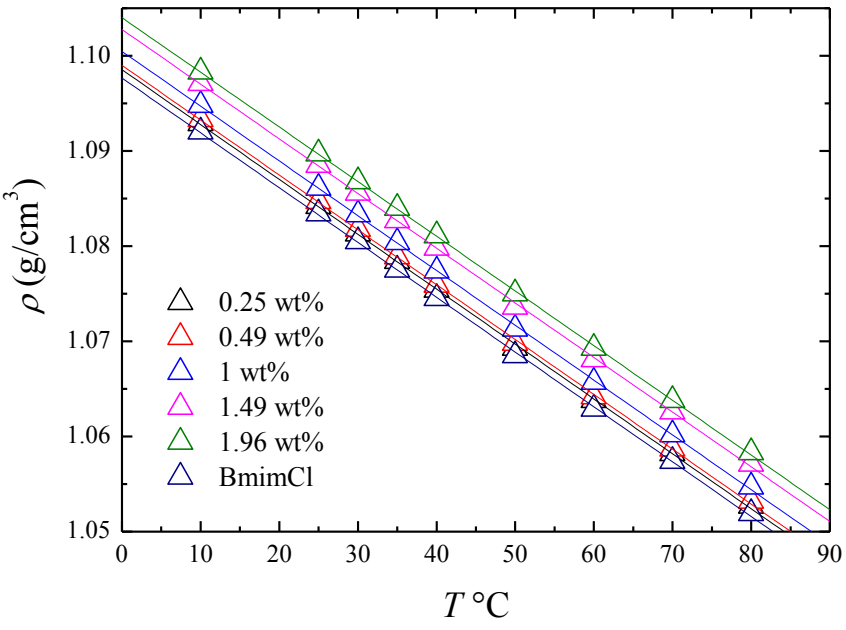

Figure 2-2-a. Temperature dependence of the density for cellulose/BmimCl solution with several concentrations.

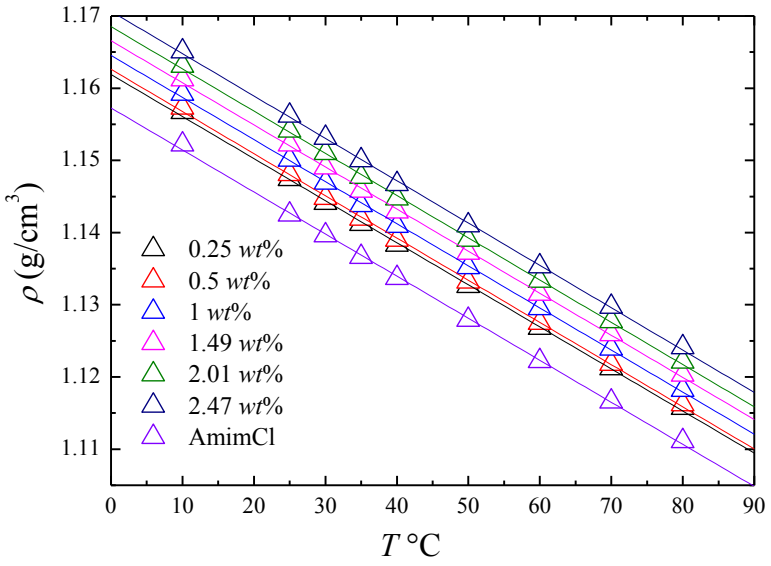

Figure 2-2-b. Temperature dependence of the density for cellulose/AmimCl solution with several concentrations.

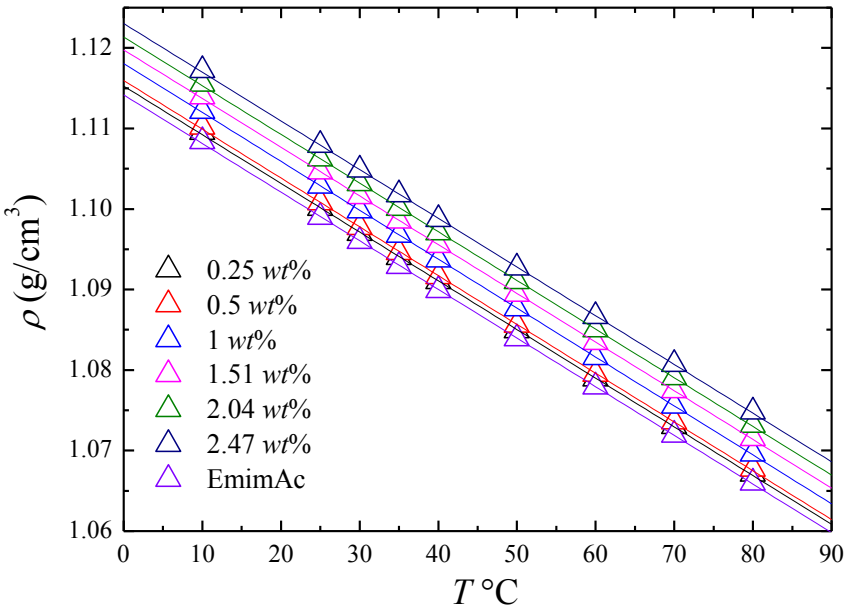

Figure 2-2-c. Temperature dependence of the density for cellulose/EmimAc solution with several concentrations.

Table 2-4. Prefactor α in eq. (1) for the cellulose/ILs solution from T = 10.00 °C to T = 80.00 °C

	α		
T	Cellulose/BmimCl	Cellulose/AmimCl	Cellulose/EmimAc
10.00 °C	3.14×10^{-3}	5.92×10^{-3}	3.65×10^{-3}
25.00 °C	3.04×10^{-3}	6.36×10^{-3}	3.79×10^{-3}
30.00 °C	3.04×10^{-3}	5.90×10^{-3}	3.67×10^{-3}
35.00 °C	3.21×10^{-3}	6.09×10^{-3}	3.76×10^{-3}
40.00 °C	3.26×10^{-3}	6.09×10^{-3}	3.76×10^{-3}
50.00 °C	3.08×10^{-3}	6.09×10^{-3}	3.63×10^{-3}
60.00 °C	3.16×10^{-3}	6.09×10^{-3}	3.60×10^{-3}
70.00 °C	3.00×10^{-3}	6.09×10^{-3}	3.69×10^{-3}
80.00 °C	3.08×10^{-3}	6.00×10^{-3}	3.69×10^{-3}

Table 2-5. Prefactor b in eq. (3) for the cellulose/ILs solution for several concentrations.

Cellulose/BmimCl		Cellulose/EmimAc		Cellulose/AmimCl	
c	b	c	b	c	b
0.00 *wt*%	$-8.55. \times 10^{-5}$	0.00 *wt*%	-8.07×10^{-5}	0.00 *wt*%	-6.24×10^{-5}
0.49 *wt*%	-7.85×10^{-5}	0.50 *wt*%	-8.23×10^{-5}	0.50 *wt*%	-7.95×10^{-5}
1.00 *wt*%	-7.88×10^{-5}	1.51 *wt*%	-8.28×10^{-5}	1.00 *wt*%	-7.92×10^{-5}
1.49 *wt*%	-7.77×10^{-5}	2.04 *wt*%	-8.24×10^{-5}	1.49 *wt*%	-7.91×10^{-5}
1.96 *wt*%	-7.82×10^{-5}	2.47 *wt*%	-8.26×10^{-5}	2.47 *wt*%	-8.07×10^{-5}

Since ILs tend to absorb moisture easily from the air, the influence of water content on ρ are also discussed. The density influence of water content C_w in *wt*% for cellulose/ILs solutions is shown in Figures 2-3. For the cellulose/BmimCl solution, water almost does not affect the density of the solution for the samples in the C_w range. It can be considered that water content has no influence to the density of cellulose/BmimCl solutions, since all the solutions in this study are not higher than 3 *wt*%.

The similar results are obtained from cellulose/AmimCl and cellulose/EmimAc solution. In this study, C_w in cellulose/AmimCl cellulose/EmimAc solutions are lower than 3 *wt*% so that the influence of water content is also negligible.

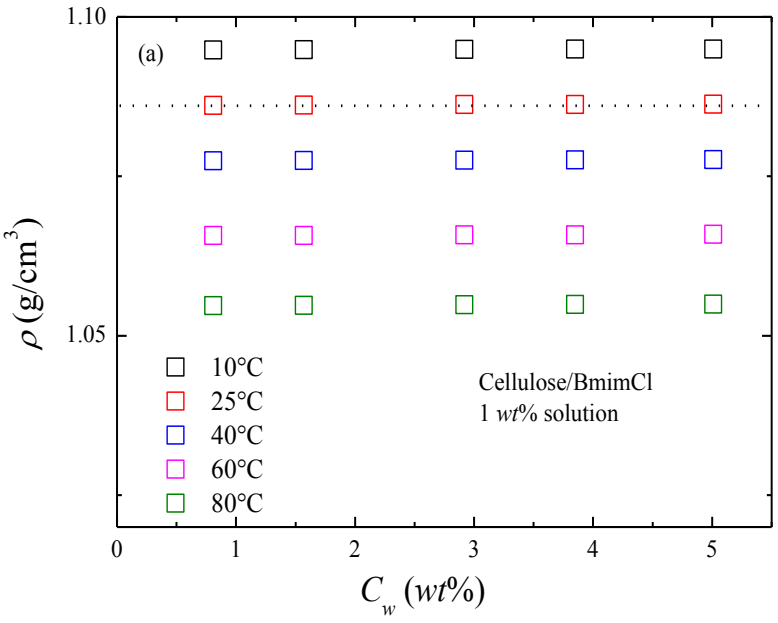

Fig 2-3-a. Water content C_w dependence of the density for cellulose/BmimCl solution at different temperature.

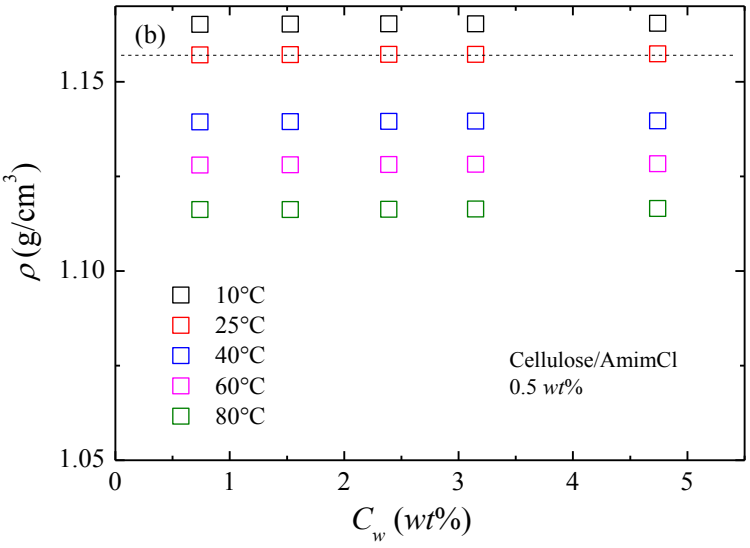

Figure 2-3-b. Water content C_w dependence of the density for cellulose/AmimCl solution at different temperature.

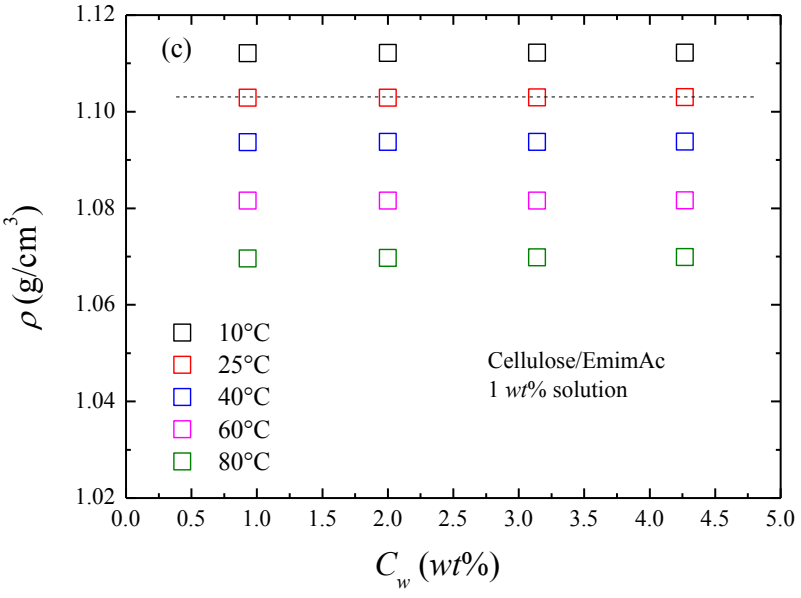

Figure 2-3-c. Water content C_w dependence of the density for cellulose/EmimAc solution at different temperature.

The density of the cellulose/BmimCl, AmimCl, EmimAc were measured in linear increasing concentration relationship of cellulose varied from dilute to concentrated region up to 2.5 *wt*%. The concentration c in wt% can be converted to C in g/cm^3 which will play an important supplementary function database for the rheological properties of the cellulose/ILs solutions by using the density results.

2.7.2 Solvent viscosity

It is known that the ILs adsorbs moisture strongly. Maruyama reported that the viscosity of BmimCl decrease with the increasing water content.[13)] Zero shear viscosity η^0 of pure ILs are measured by MCR-300 by dynamic and/or steady mode with different water contents measured at 10, 25, 40°C. The results are summarized in Figure 2-4.

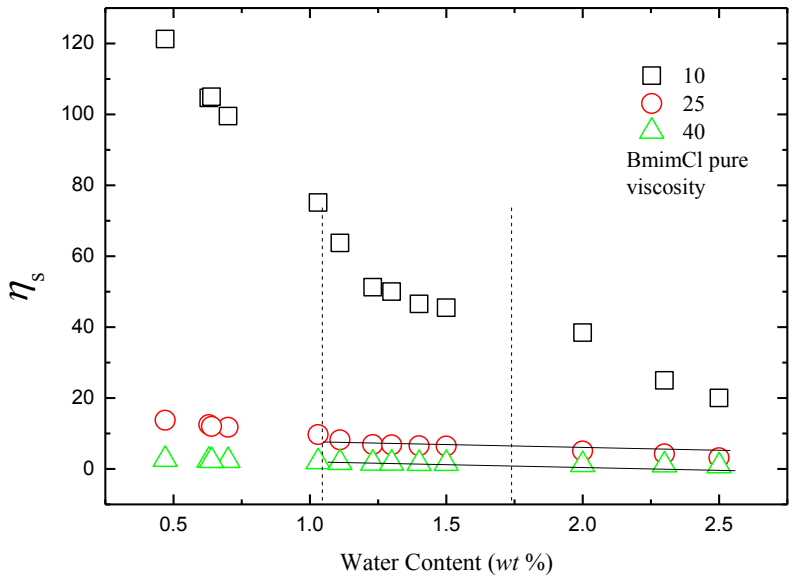

Figure 2-4-a. Water content C_w dependence of the solvent viscosity for BmimCl at different temperature.

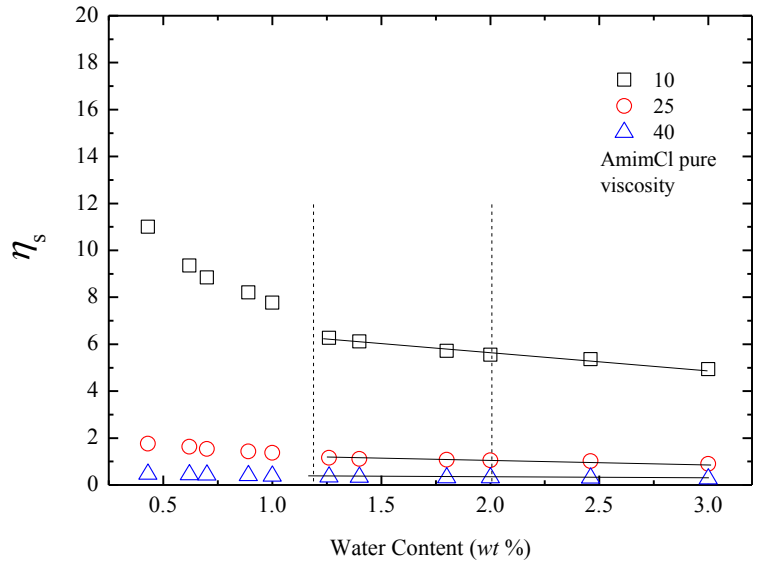

Figure 2-4-b. Water content C_w dependence of the solvent viscosity for AmimCl at different temperature.

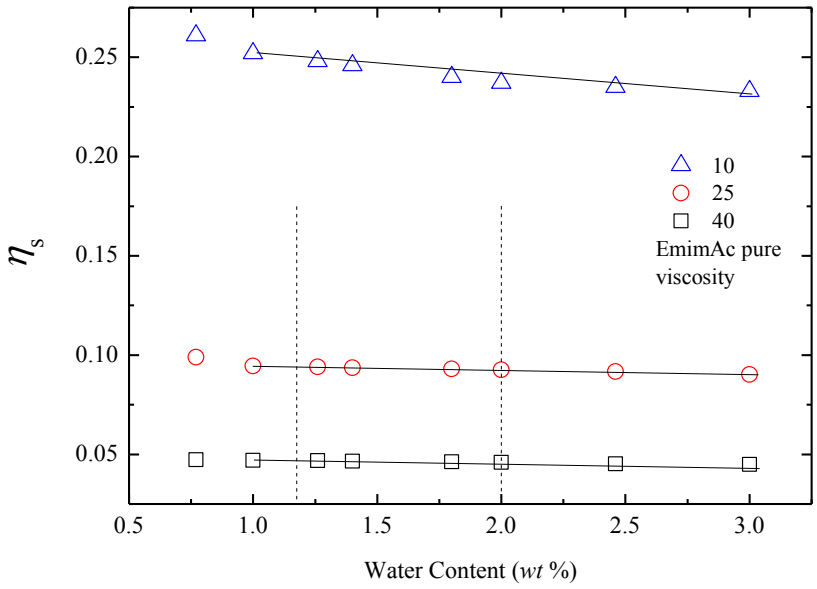

Figure 2-4-b. Water content C_w dependence of the solvent viscosity for AmimCl at different temperature.

It is clear that all the solvent viscosity change only slightly except at 10°C with low water content. These data can be used to determine solvent viscosity of the solutions since water content of our samples range in 1.2 *wt*% to 2 *wt*%, as shown by two dotted lines.

2.8 Reference

1) Fredlake C P, Crosthwaite J M, Hert D G, Aki SNVK, and Brennecke JF, *J. Chem. Eng. Data*, **49**, 954-964, 2004.

2) Sastry S, *Nature,* **409**, 164-167, 2001.

3) Lapasin R, Pricl S, "*Rheology of industrial polysaccharides: theory and applications"* (1995). Blackie Academic and Professional, Glasgow.

4) Ferry JD, "*Viscoelastic Properties of Polymers*", 3rd ed, (1980), John Wiley & Sons Inc, NY.

5) Li W, Zhang Z, Han B, Hu S, Xie Y, and Yang G, *J. Phys. Chem. B*, **111**, 6452−6456, 2007.

6) Yang Q, Zhang H, Su B, Yang Y, Ren Q, and Xing H, *J. Chem. Eng. Data,* **55**, 1750–1754, 2010.

7) Wu D, Wu B, Zhang Y M, and Wang H P, *J. Chem. Eng. Data,***55**, 621–624. 2010.

8) *Ion Ekitai (Ionic liquids)* Ⅱ; Ohno, H., ED.;**CMC** Shuppan: Tokyo (2006**)**

9) Yamamuro O, Minamimoto Y, Inamura Y, Hayashi S, Hamaguchi H, *Chem. Phys. Lett.* **423**, 371, (2006).

10) Zhang H, Wu J, Zhang J, He J, *Macromolecules,* **38**, 8272–8277 (2005).

11) Hu H, Takada A and Takahashi Y, *Evergree*n, **1**, 14-19 (2014).

12) Hu H, Takada A and Takahashi Y, *Nihon Reoroji Gakkaishi,* **42**, No.3, 191-196 (2014).

13) Maruyama E, *Physical property evaluation of BmimCl solution. Master thesis*, Department of Molecular & Material Sciences, IGSES, Kyushu University (2010).

Chapter 3 Dissolution Process of Different Kinds of Cellulose into ILs

3.1 Introduction

In this section, effects of temperature, mechanical stirring, atmosphere, and pressure on the dissolution process for four representative celluloses; avicel, cotton, nadelholz sulfur pulp (NSP), and linter pulp into BmimCl, AmimCl, and EmimAc are examined. Uniform dissolution in appearance and change in color of solution denoting oxidation and/or thermal degradation are judged by eyes. Dynamic viscoelastic properties of the solutions were measured to examine uniformity of solutions and the difference in molecular weight of samples through relative viscosity at the fixed concentration. In addition, microscopic observation was carried out at representative stages during dissolution process.

3.2 Results and discussion

Prescribed amounts of the cellulose samples and ILs are weighed and mixed into vial bottles under N_2 atomosphere in a nitrogen box to prepare 1.5 *wt*% solutions (total weight: 3 g). The mixtures are kept in a vacuum oven connected to a diaphragm pump and dissolved at 130 °C in BmimCl, 110 °C in AmimCl and 60 °C in EmimAc, at approximately 0.1 atm until the concentration fluctuation cannot be observed by eye. A few other conditions are employed to further examine the dissolution process as specified later. During the process, vacuum oven was occasionally purged by N_2 gas to observe the appearance of the solutions and to prepare samples for microscopic

observation and then heating in vacuum oven was continued. The samples for microscopic observation (ca. 3 mg each, 3 to 5 samples per a solution) were collected on a slide glass and shielded by a cover glass.

3.2.1 Macroscopic observation

Figure 3-1 shows the change of color along with heating time for cotton dissolved in BmimCl at 130 °C in *vacuo*. Figure 3-2 shows typical macroscopic observations during dissolution process for cotton/BmimCl at 130 °C, 0.1 atm. As shown in Figure 3-2-a, bubbles start to come out when the fibers start to dissolve. As shown in Figure 3-2-b, even after the solutions turned to transparent, it is still not uniform so that low viscous part and gel-like or much concentrated portions are observed when the sample vial is tilted. As shown in Figure 3-2-c, the whole solution gradually become uniform judged by the smooth flow of whole samples by continuous heating. The change of color can be more suppressed by pre-heat treatment (Fig 3-2-d) than continuous heating (Fig 3-2-c).

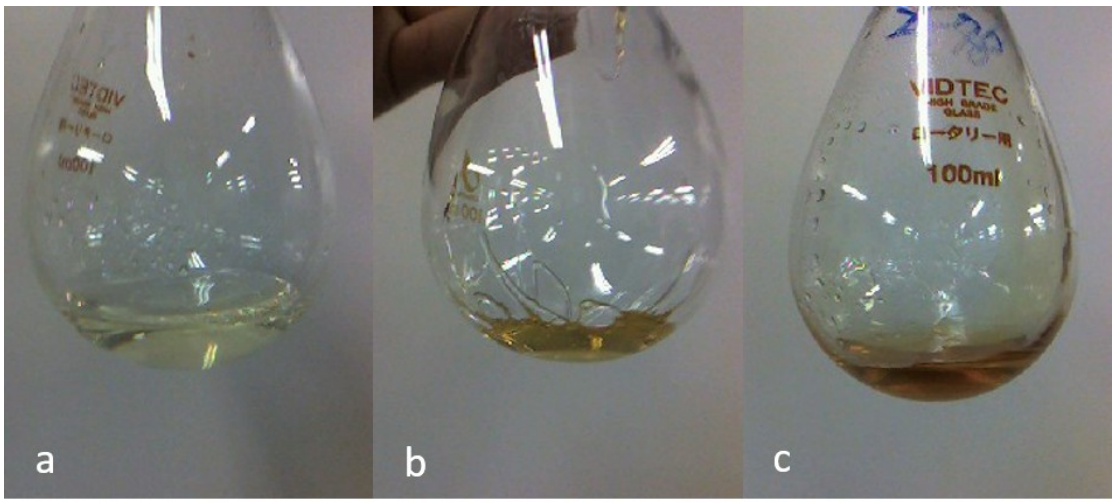

Figure 3-1. Change in sample color along heating time for cotton/BmimCl heated at 130°C in v*acuo* for (a) 1 hour, (b) 2 hours(middle), and (c) 6 hours.

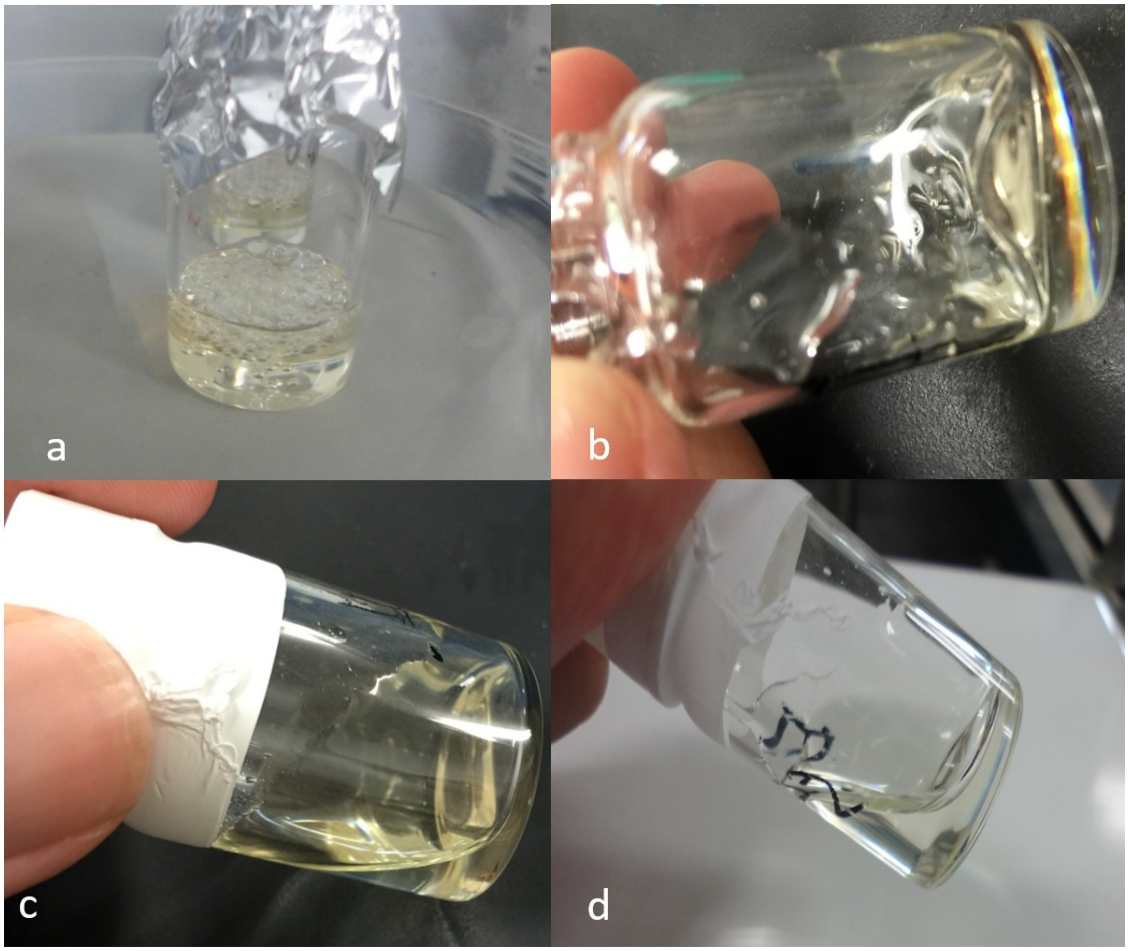

Figure 3-2. Macroscopic observations of dissolution process for cotton/BmimCl sample heated at 130 °C, 0.1 atm. a; At the beginning bubbles burst in the system and the sample turns to transparent. b; After 60 min heating, the sample have low viscous portion and high viscous portion. c; After 240 min heating, sample became macroscopically uniform solution. d; Sample dissolved with pre-heat treatment.

3.2.2 Microscopic observation

Figure 3-3 shows the structures of four kinds of cellulose samples observed by microscope. Avicel is aggregation of small pieces of microcrystalline. The length of cellulose fibers is in the order of cotton > NSP > linter pulp. A few small branches are observed for linter pulp fibers. Note that contrast and brightness of each picture are selected to focus on the structure of the samples. By changing the condition of observation, the background of picture altered one by one.

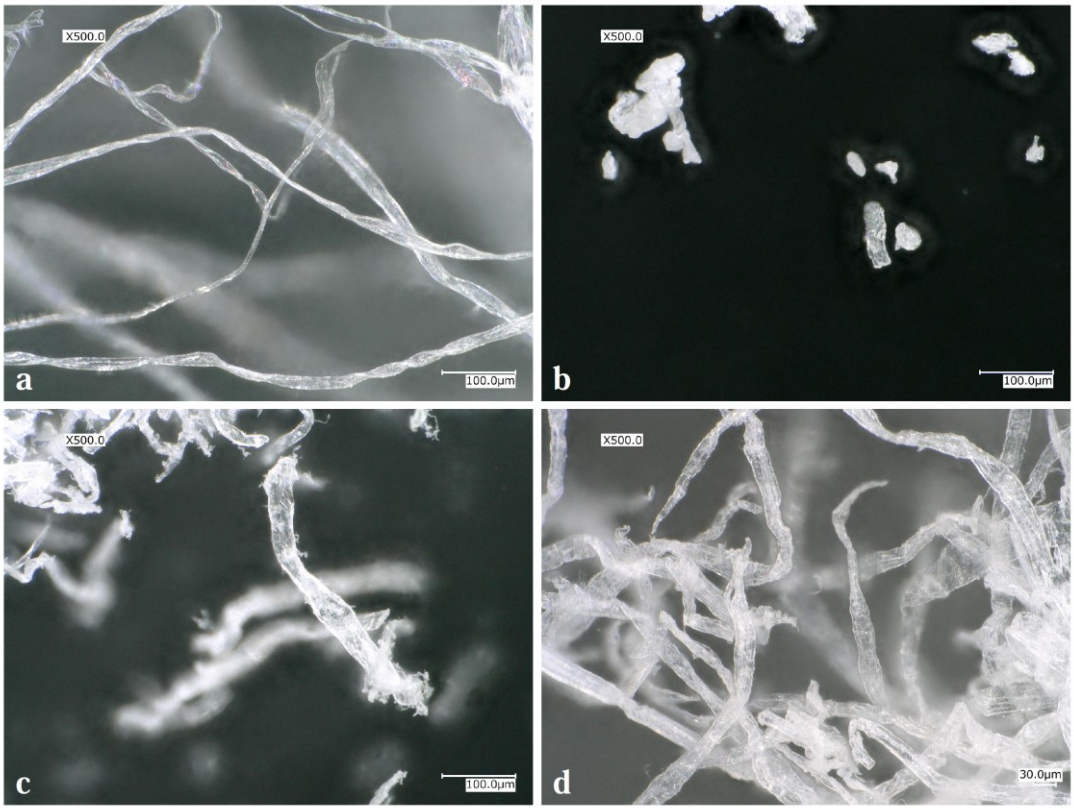

Figure 3-3. Observation under microscope; a. cotton, b. avicel, c. linter pulp, d. NSP

Figure 3-4 compares early stage of dissolution for cotton, linter pulp and NSP after 10 minutes heating at 130 °C, 0.1 atm in BmimCl. The observation for cotton/EmimAc after 5 minute heating at 60 °C, 0.1 atm is also shown. Cotton in BmimCl maintain fiber structure but other 2 samples are broken into small pieces. All observable fibrils seems to be more or less swollen. On the other hand, cotton dissolves into EmimAc very rapidly without swelling, resulting in violent bubble burst.

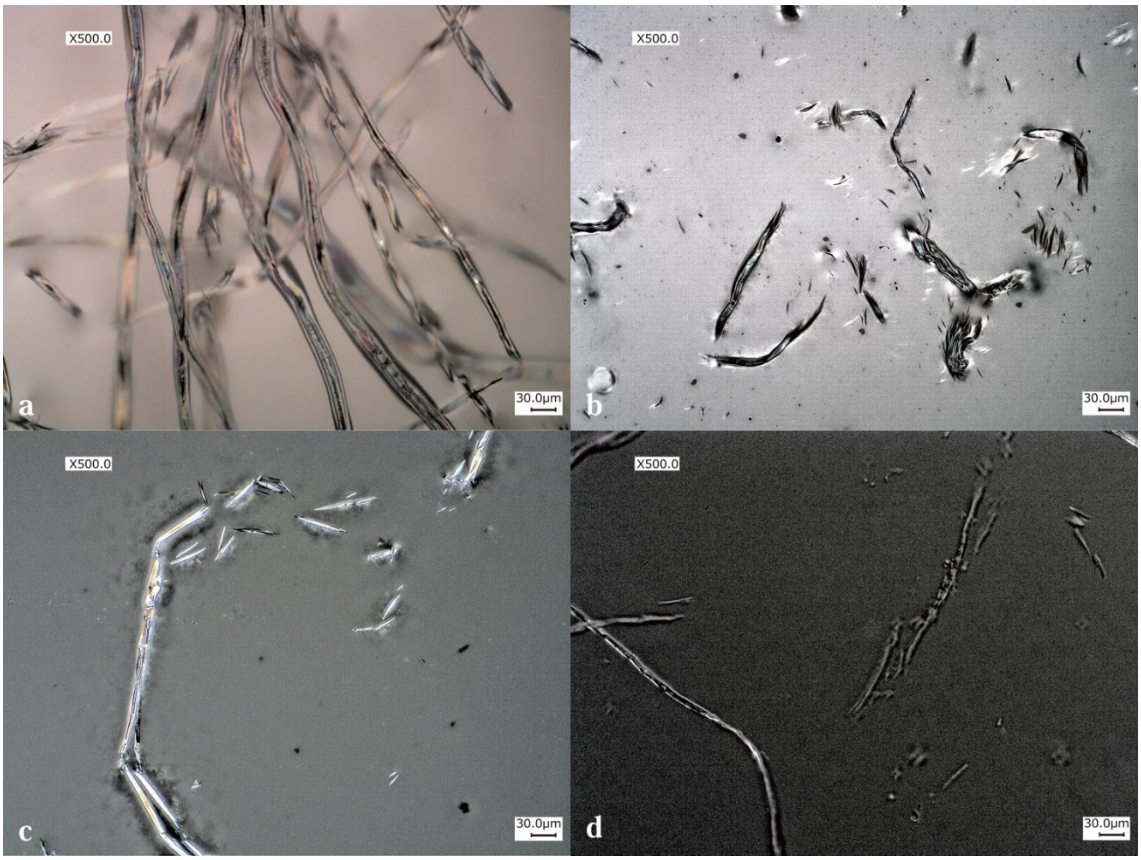

Figure 3-4. Microscopic observations after 10 minutes heating for a; cotton, b; linter pulp, c; NSP in BmimCl at 130 °C, 0.1 atm, and d; cotton/EmimAc after 5 minute heating at 60 °C, 0.1 atm.

After the samples became transparent, nothing was observed in the low viscous portion for all the samples in BmimCl and AmimCl while different structures were observed in the high viscous portion. Figure 3-5 compares structures observed in high viscous portion for cotton, avicel (translucent stuck portion), and linter. Small particles, which may be undissolved crystalline, still existed for cotton (Figure 3-5-a) and NSP (not shown). For avicel, somewhat larger micro-crystalline parts still existed (Figure 3-5-b). For linter (Figure 3-5-c), irregular gel-like particles are observed. Inside the gel-like portions, no structure was observed by the highest magnification. The number of gel-like particle diminished but the size increased with continuous heating.

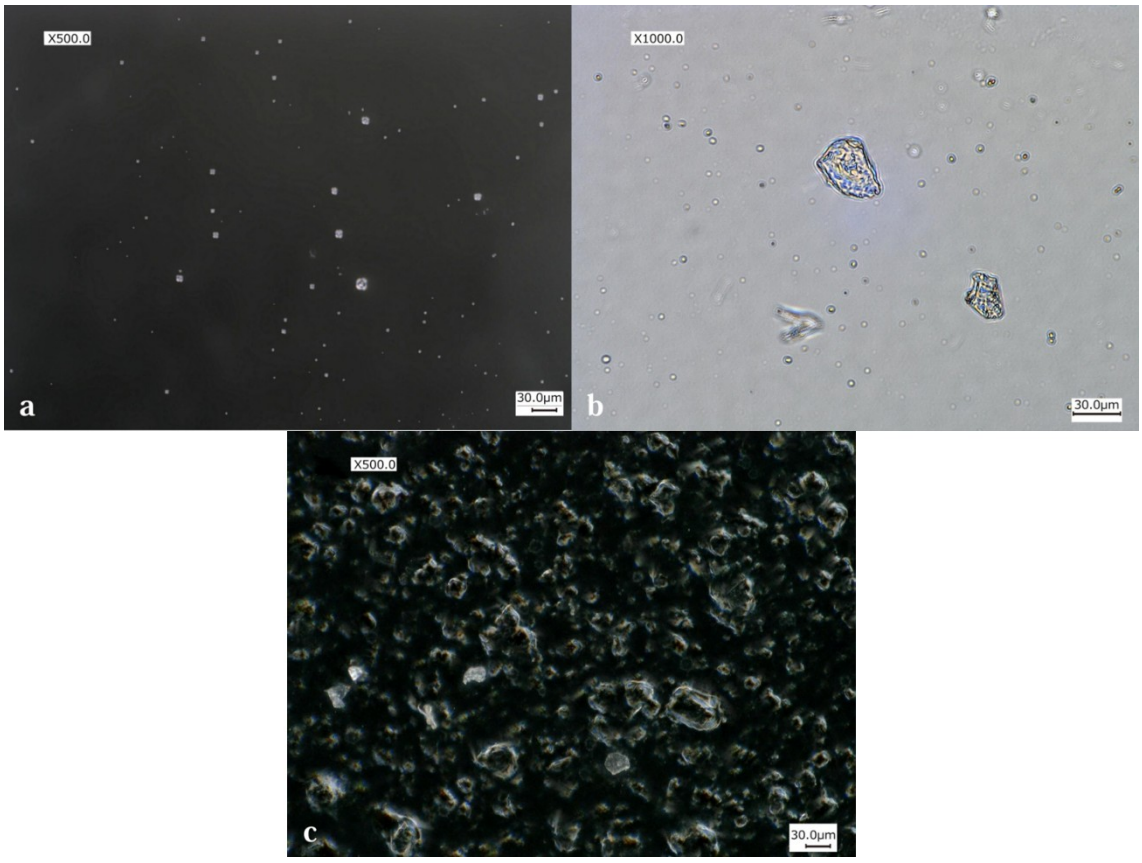

Figure 3-5. Microscopic observations for different samples in AmimCl dissolved at 110 °C, 0.1 atm. a; high viscous portion in cotton/AmimCl, b; sticky portion in avicel/AmimCl, and c; high viscous portion in linter/AmimCl.

The microscopic observations were also carried out for cotton and NSP in BmimCl pre-heated at 80 °C, 0.1 atm. As shown in Figure 3-6-a, the NSP fibers are irregularly swollen, containing non-swollen part along the fibers. By the continuous heating, the original fibers break into thinner fibers and/or smaller pieces as observed in Figure 3-6-b. The swollen parts seems to be accompanied with the most of thinner fibers and small pieces. For cotton in BmimCl (Figure 3-6-c), it was more clearly observed than the NSP that elliptically swollen parts are connected by un-swollen short and thin fibers or particles. With further heating (Figure 3-6-d), the connected swollen parts gradually broken to be isolated. It is speculated that short fibers and particles are remaining crystalline of cellulose while the swollen part is gel-like; almost dissolved cellulose chains may be still connected by very small crystalline which cannot be observed by the microscope. It is also speculated that fully dissolved cellulose chains can diffuse out from the swollen part so that the size of swollen part does not change so much during the observation. These observations are similar to the results reported for cotton in Cuprammonium hydroxide by Tripp VW *et al*[1)], cotton in NMNO water mixtures[2)] and in NaOH-Water-Additives systems (NaOH concentration at 7.6%)[3)] by Cuissinat *et al*.

From the above observation results, we can summarize the common dissolving process of cellulose samples as follows. First amorphous rich part more or less swell while crystalline rich part dissolve into ILs gradually, being non-uniform solution. The swollen parts may still contain microcrystalline which is not observable by microscope. Both the observable crystalline and non-observable microcrystalline continuously dissolve into ILs and fully dissolved chains become molecularly dispersed in the solution and finally approach the uniform stage. The difference in the observation for different samples may come from various reasons such as differences in chemical and physical treatment during the purification of cellulose, remaining impurities, degree of

crystallinity and so on. Basically, the above process is consistent with that reported by Kosan *et al*.[4), 5)] They reported that cellulose/IL mixture first turns to be gel-like during the dissolving process in kneader. With continuous heating and mixing in *vacuo*, the solution finally turns to be uniform.

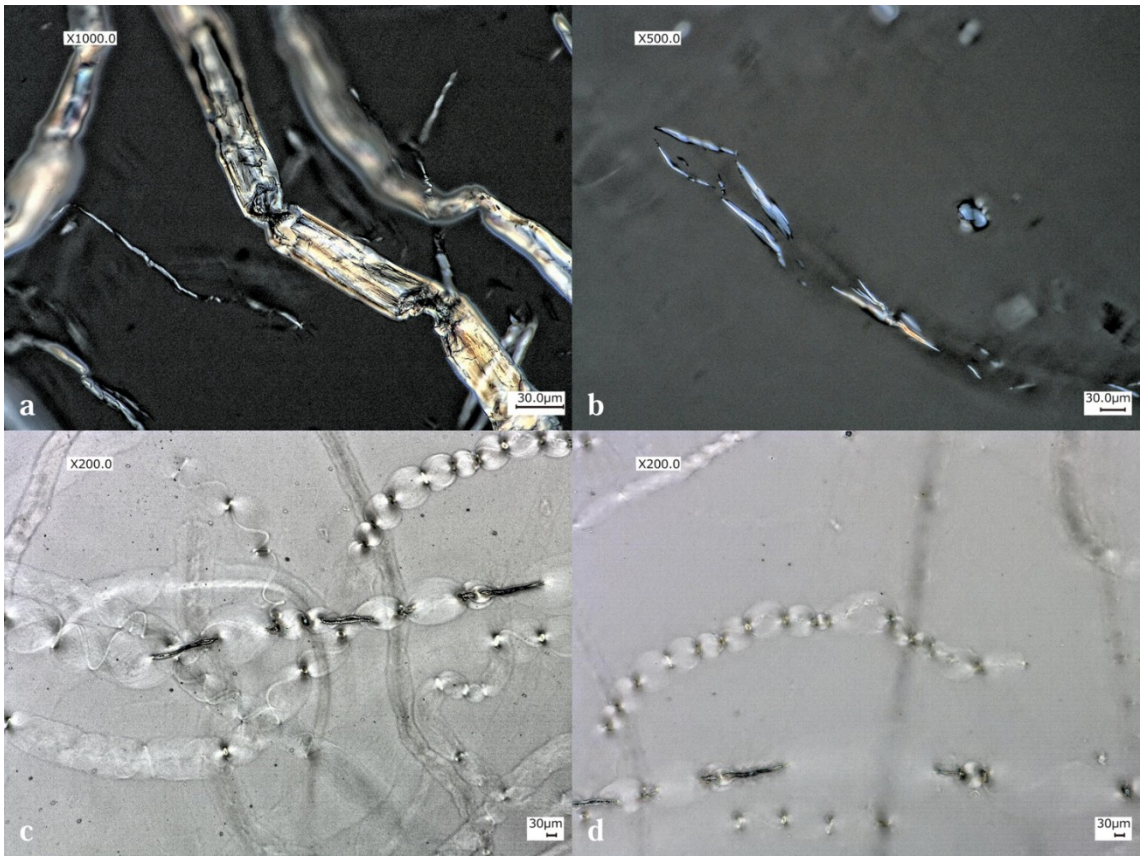

Figure 3-6. Microscopic observations for samples heated in BmimCl at 80 °C, 0.1 atm. a; NSP after 10 minutes heating, b; NSP after 60 minutes heating, c; cotton after 240 minutes heating and d; cotton after 280 minutes heating.

3.2.3 Rheological measurements

For cotton/BmimCl solutions prepared under *vacuo*, macroscopically uniform solutions scarcely obtained at 120 °C but it was obtained after about 2 hours heating at 130 °C. Violent bubble burst was observed under this condition. Figure 3-7 shows frequency (ω) dependences of storage (G') and loss (G'') moduli for cotton in BmimCl solutions prepared under *vacuo* at 130 °C with and without mechanical stirring. Though the terminal region behavior is observed for these solutions, the solutions turned to brown quickly within 2 hours (see Fig.3-1). It is also clear that stirring results in the lower G' and G'' values. Therefore, stirring bar was not used in the following experiments.

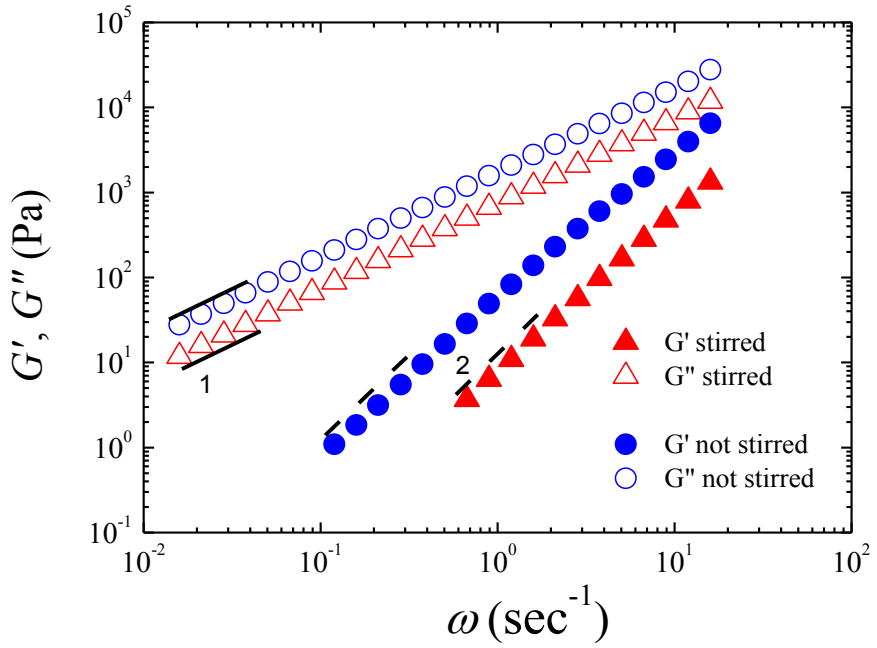

Figure 3-7. Double logarithmic plots of G' and G'' vs ω for cotton/BmimCl at 10 °C, prepared in *vacuo* at 130 °C with and without stirring. The symbols are denoted in the figure.

Dissolution temperature for cotton/AmimCl and cotton/EmimAc was examined at 0.1 atm to avoid violent bubble burst. The uniform solution for cotton/AmimCl can be attained at 90 °C after about 48 hours heating, while it took only 8 hours at 110 °C. At still higher temperature, change in the color of solution became significant.

The cotton fibril disappeared very quickly (see Fig. 3-4-d) in EmimAc at 60 – 90 °C with violent bubble burst so that part of sample spilled and stuck to upper wall of vial. Consequently, G' and G'' became very low at these conditions. The situation was not well improved under N_2 atmosphere. At the lower temperature, say 40 °C, the rheological data did not show apparent terminal region behavior. Thus, we could not find appropriate condition to further examine EmimAc system.

The dissolution of cellulose into BmimCl and AmimCl under N_2 atmosphere are examined at 130 °C and 110 °C, respectively. The bubble burst was observed for about 1.5 hours. We speculate that the origin of bubbles is bound water in cellulose. The effects of bound water will be discussed in chapter 5. The color of the solutions changed to slightly yellow after about 3 hours heating and gradually turned to brown at longer time. The NSP solutions became macroscopically uniform within the shortest heating time, say 5 hours. Figure 3-8 shows double logarithmic plots of G' and G'' vs. ω for the NSP/BmimCl solutions measured after different heating time. Since the terminal region behavior is observed for these samples, it can be concluded that NSP solution is uniform after 5 hours heating. It is clear that the G' and G'' data decrease with increase of heating time, which may mean that longer heating causes degradation of the sample.

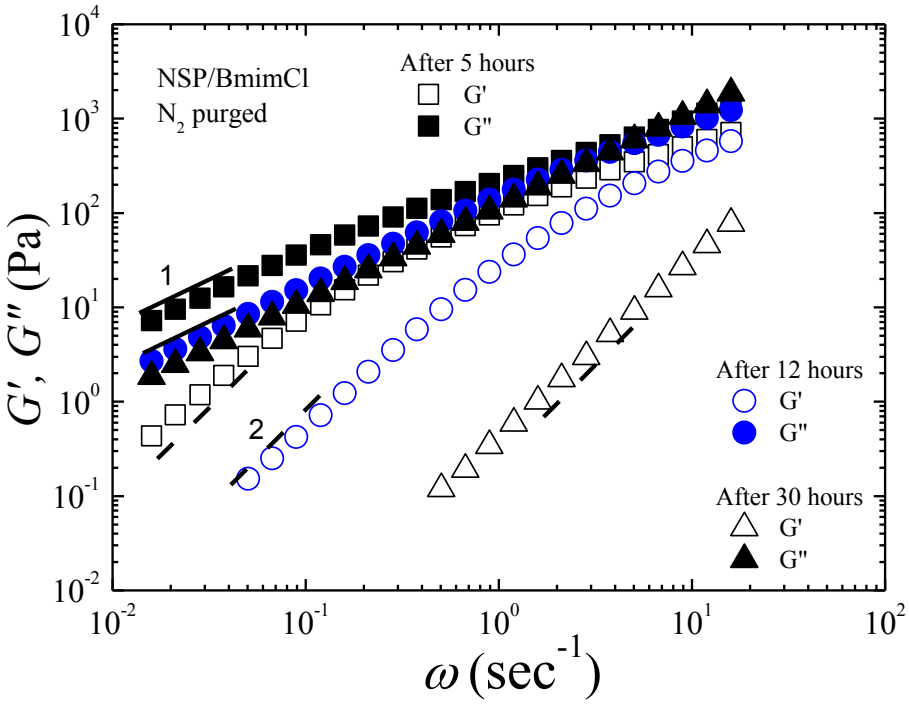

Figure 3-8. Double logarithmic plots of *G*' and *G*" vs ω measured at 25 °C for NSP in BmimCl prepared at 130 °C, 1 atm with different heating times. The symbols and are denoted in the figure. (Note that the typical terminal region behavior for 5h in low frequency region cannot be observed well)

After 12 hours heating, cotton and NSP solutions both in BmimCl and AmimCl became uniform, while some gel-like residue remained in linter solution and small amounts of avicel stuck to the bottom and wall of the vial (see Figure. 3-2). The rheological data for all the samples are summarized in Figure 3-9. Note that the measurement for linter and avicel solutions were carried out by removing non-uniform portion so that their concentrations are somewhat different from the prepared values. The data are shifted along the vertical axis to avoid overlapping. The typical terminal region behavior for viscoelastic liquids are observed for all the samples by selecting

appropriate measuring temperature. It took about 30 hours to almost completely dissolve avicel solutions, while gel-like residue in linter solution remained even after 30 hours heating.

To harmonize shorter heating time and mild bubble burst, the celluloses/BmimCl and AmimCl mixtures were dissolved under 0.1 atm. The bubble burst became mild than that in *vacuo* and observed for less than 1 hour. The color of both BmimCl and AmimCl solutions are very slightly yellow and remained almost unchanged for about 4 hours heating but the color of solutions gradually changed at longer time. The samples are more or less non-uniform at short heating time (see Figures. 3-4 ~ 3-5). Uniform solutions for cotton and NSP was obtained after about 6 - 7 hours heating. It took about 12 hours to fully dissolve avicel. For linter/ILs solutions, gel-like residues still existed. When the linter solutions were further kept at 60 °C in an oven for 3 days to suppress degradation, the gel-like portions still remain undissolved. Figure 3-10 summarize the *G*' and *G*" data for all the solutions in BmimCl (the gel was removed from linter/ILs for the measurement). The results for AmimCl solutions are compared with others in Figure 3-12.

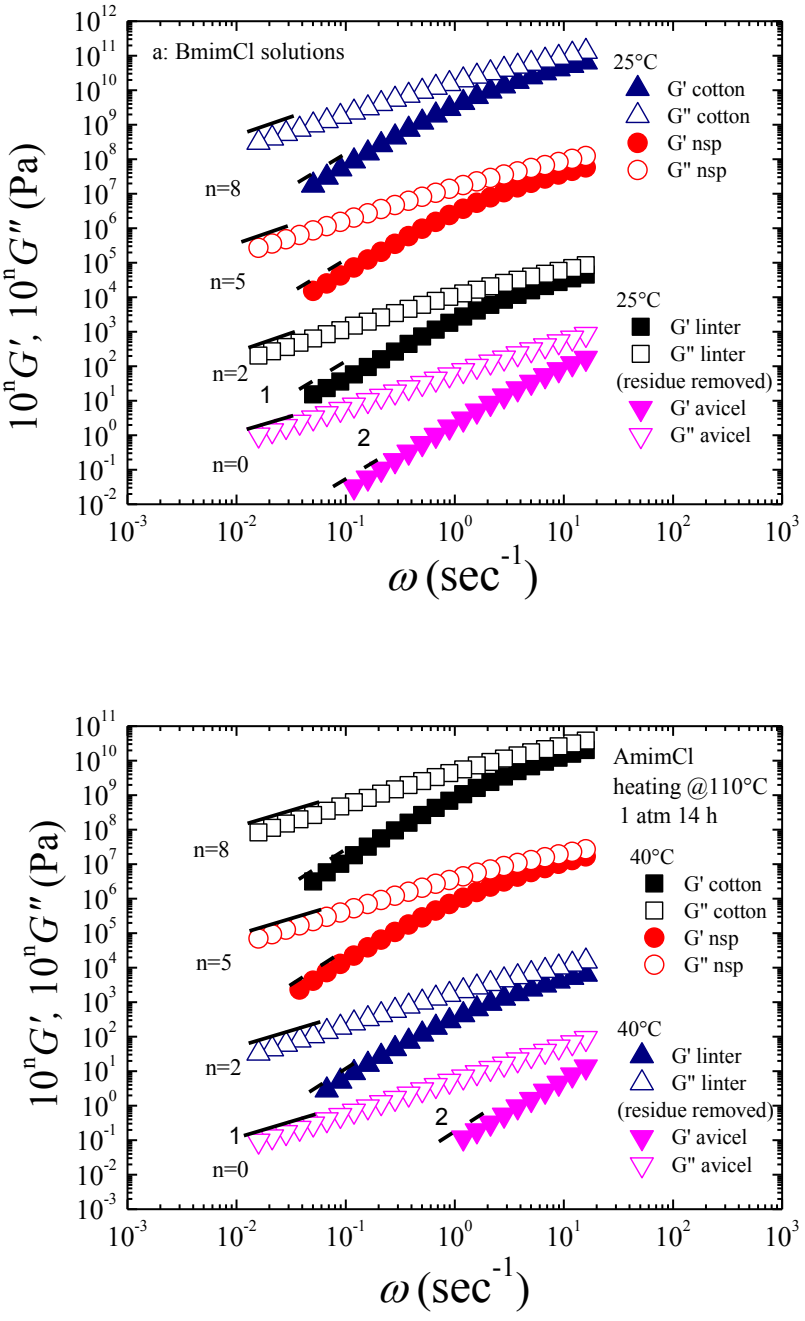

Figure 3-9. Double logarithmic plots of *G*' and *G*" vs ω for cellulose solutions prepared under 1 atm N_2 in BmimCl at 130 °C 1 atm and in AmimCl at 110 °C. Symbols and measuring temperatures are denoted in the figure.

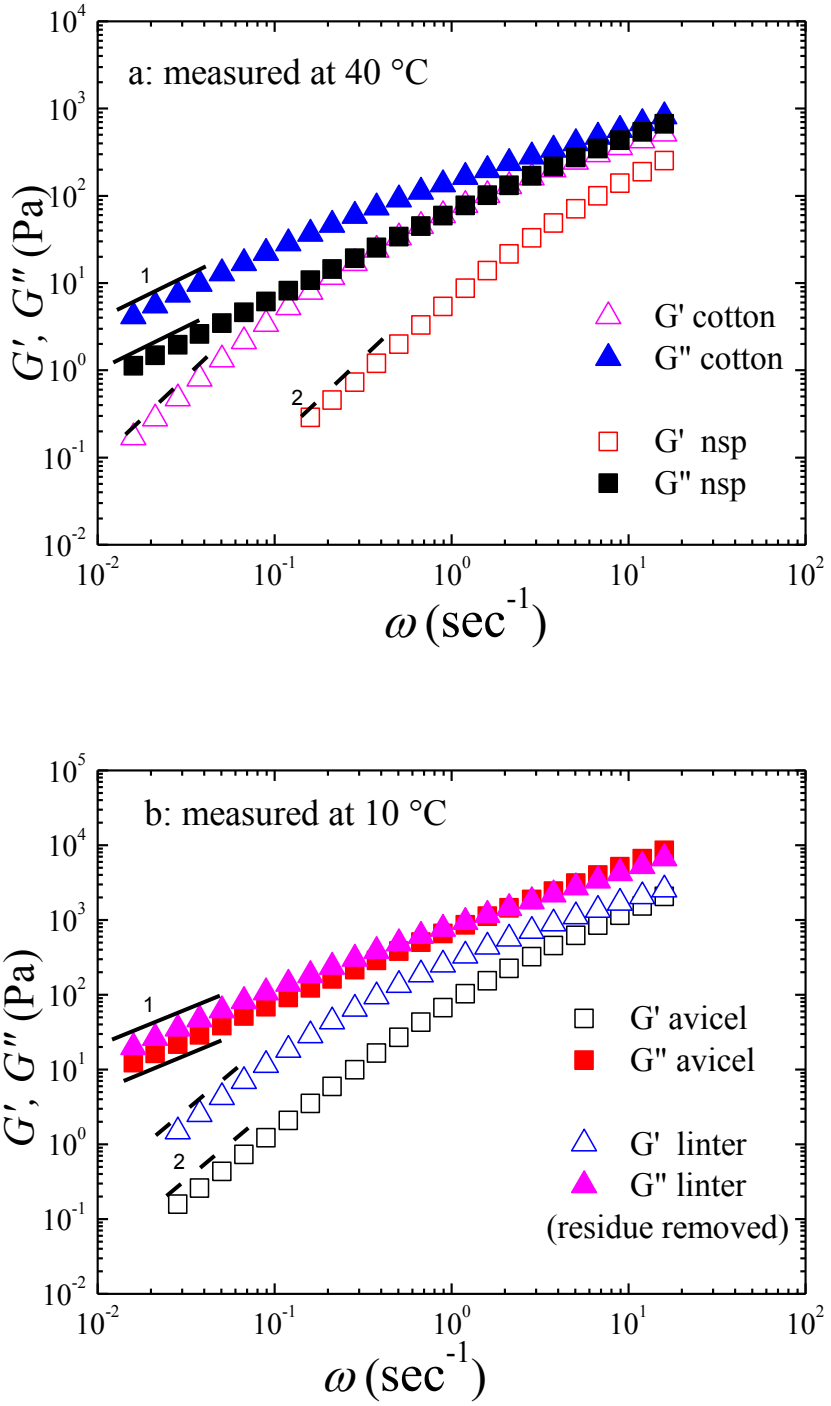

Figure 3-10. Double logarithmic plots of *G*' and *G*" vs ω for a; cotton and NSP and b; avicel and linter in BmimCl prepared at 130 °C 0.1 atm. The symbols and measuring temperatures are denoted in the figure

In order to seek more mild dissolution condition, pre-heating of the samples at 80 °C, 0.1 atm in BmimCl are tested for cotton and NSP. At this condition, the bubble bursting speed fairly diminished. Under this heating condition, irregularly swollen fibers can be observed, which seems to be dissolving very slowly and small crystalline parts was still observed under microscope even after 48 hours heating. Since NSP fibers more easily break into thinner and shorter ones than cotton fibers, further experiment was carried out only for cotton. That is, the cotton was heated at 80 °C, 0.1 atm for 4 hours in BmimCl and then dissolved at 130 °C by 2 hours heating. Then the samples are purged by N_2 gas and kept in an oven at 60 °C for 7 – 10 days until concentration fluctuation cannot be observed by eye. During this process, vial bottles are occasionally tilted and/or rotated. The solution color became almost unchanged by this procedure (see Appendix Fig. 3-2-d). Figure 3-11 compares the *G*' and *G*" data for cotton/BmimCl dissolved at 130 °C, 0.1 atm with and without pre-heating. It is clear that *G*' and *G*" for pre-heated solution are higher than those without pre-heating.

There is a possibility that cellulose chains in the solutions, whose terminal region behavior is apparent, are still not molecularly dispersed due to remaining non-observable microcrystalline. Therefore, we purged cotton/AmimCl solution (dissolved at 110 °C, 0.1 atm) with N_2 gas and kept at 60 °C to examine further change of data. Note that cellulose swells at this temperature in AmimCl. The data remain unchanged after 3 months storage. Thus, we conclude that the cellulose chains are molecularly dispersed in the solution. The difference in viscoelastic data reflects the difference in molecular weight of samples.

To compare the data at different temperatures, we use $\eta_r = \eta^0/\eta_s$ (η_s: solvent viscosity) since they are measured at almost the same concentration. Here, we simply assume that the solvent power is the same at different temperatures and η_s values can

be determined by taking into account of the initial water content of ILs[4]. The evaluated η_r values are summarized in Figure 3-12. It is clear that the cotton solution preheated at 80 °C for 4 hours then dissolved at 130 °C under 0.1 atm shows high molecular weight than those prepared without preheating under different conditions.

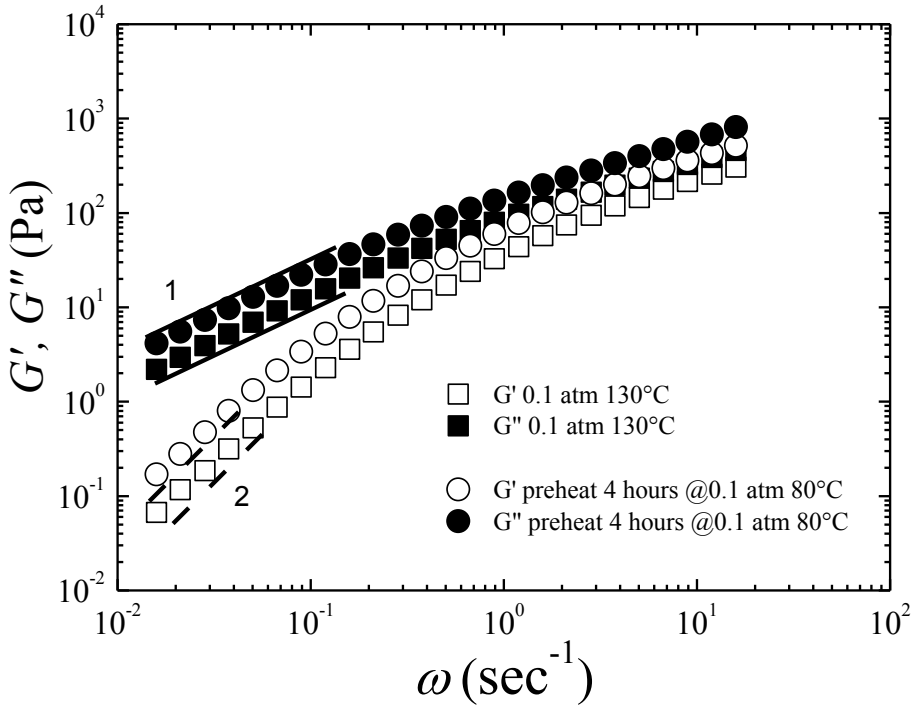

Figure 3-11. Double logarithmic plots of *G*' and *G*" vs ω measured at 40 °C for cotton directly dissolved into BmimCl prepared at 130 °C 0.1 atm, preheated at 80 °C 0.1 atm for 4 hours then dissolved at 130 °C 0.1 atm for 2 hours. The symbols are denoted in the figure.

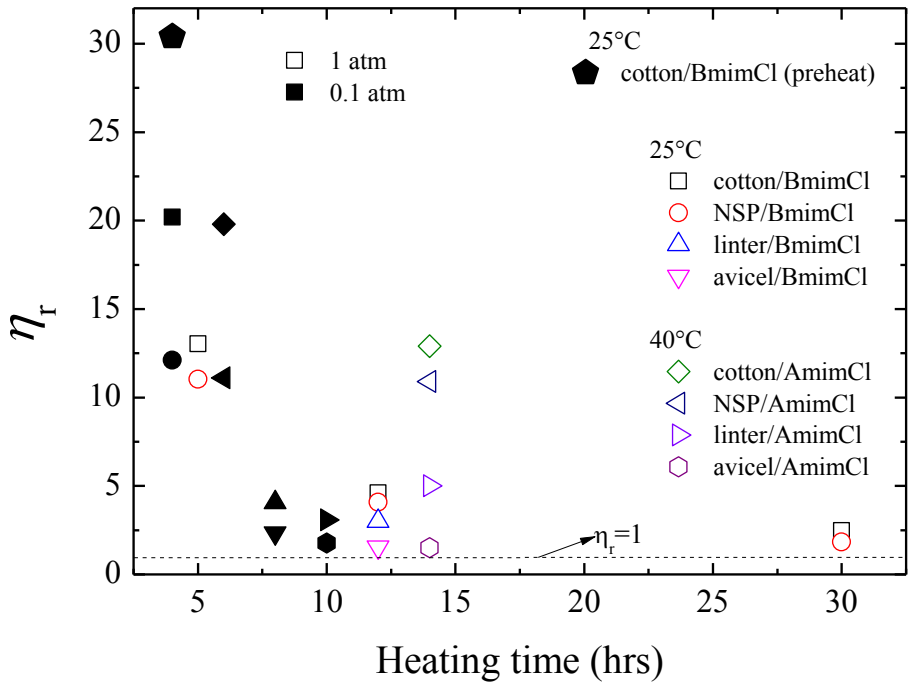

Figure 3-12. Plots of heating time vs η_r for celluloses/ILs measured at different times. BmimCl solutions are dissolved at 130 °C and AmimCl solutions are dissolved at 110 °C. Symbols and measuring temperatures are denoted in the figure.

From above results, we conclude that the tested dissolution processes are inadequate for EmimAc. It is also difficult to obtain colorless and totally uniform solutions for avicel and linter in BmimCl and AmimCl. Cotton and NSP can be dissolved uniformly into BmimCl and AmimCl. The difference in the samples may come from different origins and different pre-treatments of them. It is essential to control bubble burst speed by preheating and keep the solution at lower temperature to get almost colorless and high viscosity uniform solutions. More systematic experiments for dissolution condition, as well as reproducibility of data should be needed to further

examine the applicability of cellulose/IL solutions for characterization methods and/or control of molecular weight of cellulose by changing dissolution condition.

3.3. Summary

We examined dissolution conditions of avicel, cotton, nadelholz sulfur pulp (NSP), and linter pulp into 1-butyl-3-methylimidazolium chloride (BmimCl), 1-allyl-3-methylimidazolium chloride (AmimCl) and 1-ethyl-3-methylimidazolium acetate (EmimAc) to obtain less damaged (less colored and higher viscosity) uniform solutions. The tested dissolution conditions are inadequate for EmimAc. To suppress degradation of cellulose, depressed conditions without mechanical stirring are effective for BmimCl and AmimCl systems. Under those conditions, cotton and NSP can be dissolved uniformly with less change in the color but avicel and linter cannot be. When the bubble burst was suppressed by pre-heating, color change of solution was more suppressed. The pre-heated cotton solution showed higher relative viscosity than others.

3.4. Reference

1) Tripp VW, Rollins ML *Anal.Chem*., **24**, 1721 (1952).

2) Cuissinat C, Navard P, *Macromol.Symp*., **244**, 1 (2006).

3) Cuissinat C, Navard P, *Macromol.Symp*., **244**, 19 (2006).

4). Kosan B, Michels C, Meister F, *Cellulose*, **15**, 59-66 (2008).

5) Kosan B, Schwikal K, Meister F, *Cellulose*, **17**, 495-506 (2010).

6) Hu H, Takada A, Takahashi Y, *Nihon Reoroji Gakkaishi* **42**, No.3, 191-196 (2014).

Chapter 4 Molecular Weight Estimation of Cellulose in ILs Solutions

4.1 Introduction

To study cellulose/ILs solutions more systematically, it is essential to compare the molecular weights of samples prepared at different conditions. In this section, we examine molecular weight estimation of cellulose in ILs by fitting dynamic viscoelastic data to Rouse-Zimm (RZ) model with a correction term called long time (LT) term examined for standard polystyrene samples by Osaki *et al*[1]. The data are first fitted to RZ model by using molecular weight M as a parameter, while fixing other parameters. Then the LT term, calculated from intrinsic viscosity $[\eta]$ and two adjusting parameters, is employed to judge the appropriateness of the estimation of molecular weight.

4.2 Result and discussion

4.2.1 Intrinsic viscosity of cellulose/AmimCl solutions

AmimCl and cellulose were dried in *vacuo* at 60 °C for 12 hours, then prescribed amounts of them are weighed and mixed into PFA vials under N_2 atmosphere in a nitrogen-box. Three different sample solutions, T1 (1.02 *wt*%), T2 (0.986 *wt*%), and T3 (0.868 *wt*%) are prepared. The mixtures are kept at 60°C under 0.1 atm N_2 atmosphere for 1 hour then kept at 100°C under 0.2 atm N_2 for 2 hours. After the samples became transparent, they are kept heating at 60°C under 0.1 atm N_2 for 48

hours to fully remove the bubbles. Then the solutions are purged by N_2 and kept in an oven at 60°C. The vial bottles are occasionally titled or rotated until concentration fluctuation disappeared.

Some portion of original solutions are transferred to PFA vials in a nitrogen-box and diluted to prepare lower concentration samples. The diluted solutions are treated by similar manner as mentioned above to obtain uniform solutions. All the samples are dried in *vacuo* at 60 °C for 12 hours before the measurement. The water content of the solutions just before the measurement was determined by Karl-Fisher titration (KEM, MKC-501). Concentration of the solutions c (*wt*%) are converted to C (g/cm^3) by using empirical relationships obtained in chapter 2.

Zero shear viscosity η^0 of diluted solutions are also measured by MCR-300 by dynamic and/or steady mode at 40°C. Relative viscosity, $\eta_r = \eta^0/\eta_s$, and specific viscosity, $\eta_{SP} = (\eta_r - 1)$ are obtained by using solvent viscosity η_s corrected for water content. Water content dependence of η_s are measured at three different temperatures by rheometer as shown in Figure 4-1. It is clear that solvent viscosity change only slightly except at 10°C with low water content. These data can be used to determine solvent viscosity of the solutions since water content of our samples range in 1.2 *wt*% to 2 *wt*%, as shown by two dotted lines.

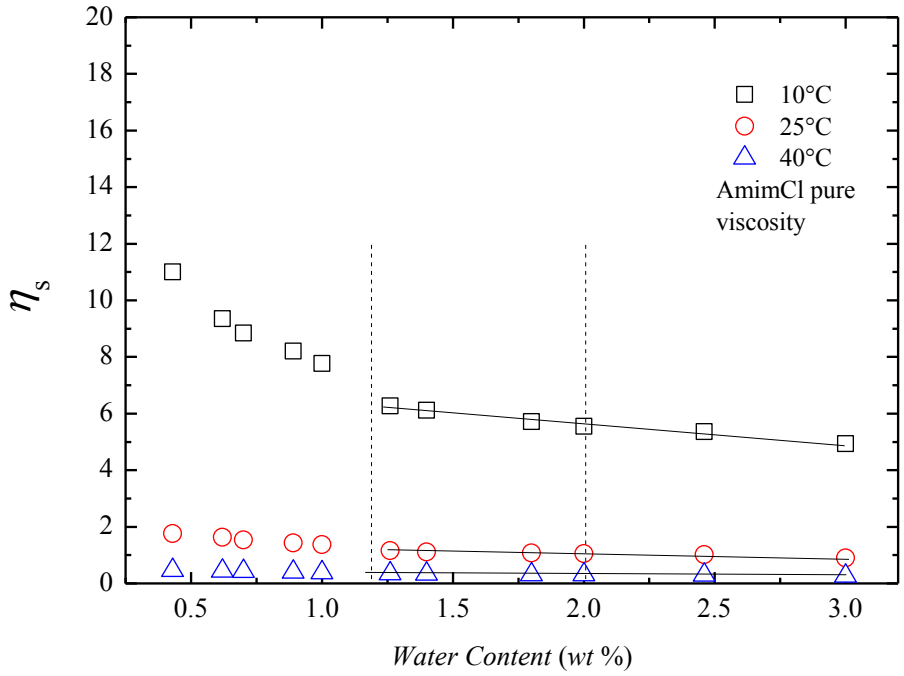

Figure 4-1. Water content dependence of solvent viscosity measured at three different temperatures. Symbols are denoted in the figure. Two dotted lines indicate usual range of water content for our experiments.

Figure 4-2 shows plots of η_{sp}/C and $\ln\eta_{rel}/C$ vs C, for diluted solutions prepared from T1, T2 and T3 at 40°C. It is clear that $[\eta]$ for each sample can be determined by extrapolation to zero concentration shown by two straight lines only with small error. From obtained $[\eta]$ and concentrations of T1, T2 and T3, we can say that these solutions are in the so-called Rouse-like region ($C[\eta] > 2.5$). Inoue *et al.*[2), 3)] reported that polymer chains are overlapped with each other at $C[\eta] > 2.5$ so that the hydrodynamic interactions are shielded at $C[\eta] > 2.5$.

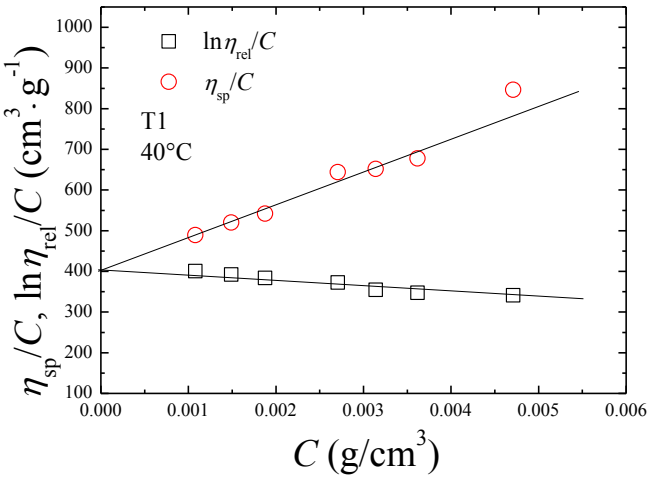

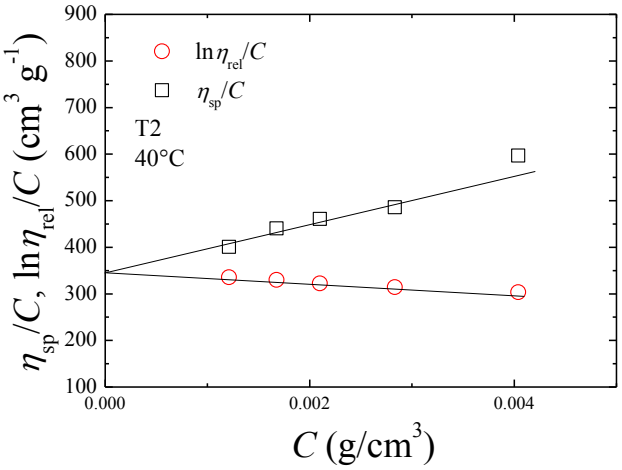

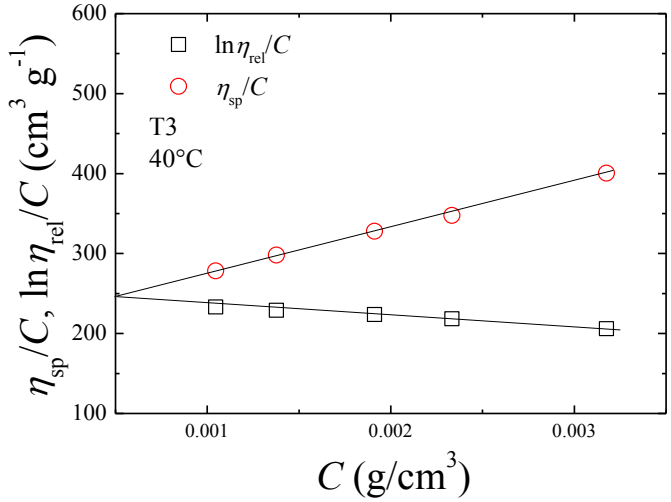

Figure 4-2. Concentration dependence of η_{sp}/C and $\ln\eta_{rel}/C$ for cellulose AmimCl solutions T1, T2, and T3 at 40 °C.

4.2.2 Estimation of cellulose/AmimCl solutions by Rouse-Zimm model

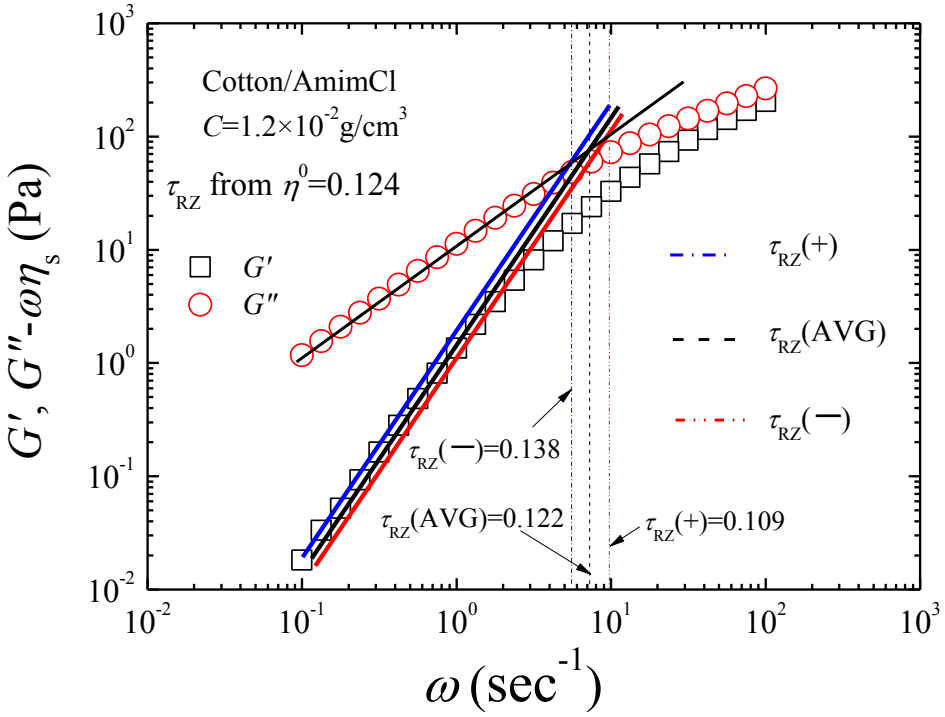

Figure 4-3. Double logarithmic plots of *G'* and *G"* vs ω for cotton/AmimCl T1 measured at 40°C. Relaxation time τ_{RZ} obtained from the crossing point of *G'* and *G"* by using different lines are designated in the figure. Symbols and other information are also denoted in the figure. The value τ_{RZ} from η^0 is obtained from Rouse model.

Figure 4-3 shows an example of double logarithmic plots of storage, *G'* and loss *G"*, moduli vs frequency ω for T1 solution at 40°C. The longest relaxation time τ_{RZ} can be phenomenologically obtained from the inverse value of ω at the crossing point of two extrapolated lines for *G*' and *G*" data in the terminal region as illustrated by a few sets of lines. The line for *G"* can be drawn without ambiguity but the line for *G*'

might be somewhat ambiguous since the slope of log G' vs ω is not exactly 2. That is, we can draw line to fit most of the data, fit the data at low ω end and alternatively at the higher portion of ω in the terminal region as shown in Figure 4-3. The first one is the modest case while two others may be the upper and the lower limit of line fitting. The estimated τ_{RZ} from the upper and the lower limit are designated as τ_{RZ}(-) and τ_{RZ}(+), respectively, while τ_{RZ} from the modest case coincide to the average of τ_{RZ}(-) and τ_{RZ}(+) so that designated as τ_{RZ}(AVE). We assume that two limiting cases show the estimation error of τ_{RZ}. We test fitting of the data with RZ model with and without LT term described below, by using above estimated τ_{RZ}s as the longest relaxation time.

The Rouse-Zimm (RZ) model can be expressed by the following general formulae,

$$G''(\omega) = \frac{CRT}{M}\sum_{p=1}^{N}\frac{\omega\ \tau_P}{1+\omega^2{\tau_P}^2} + \omega\eta_s \qquad (1)$$

$$G'(\omega) = \frac{CRT}{M}\sum_{p=1}^{N}\frac{\omega^2{\tau_P}^2}{1+\omega^2{\tau_P}^2} \qquad (2)$$

$$\tau_p = \frac{\tau_{RZ}}{p^{\alpha}} \qquad (3)$$

where R is the gas constant, T is the absolute temperature, and τ_p is the relaxation time of pth normal mode defined in eq.3 with τ_{RZ}. The hydrodynamic interaction parameter α can be fixed as 2 (Rouse model) since all examined solutions are in the range $C[\eta]$ > 2.5. Osaki *et al.*[1)] employed long-time (LT) term to get better fitting at low ω region.

$$G'_{LT} = G_{LT}\frac{\tau_{LT}{}^2\omega^2}{1+\tau_{LT}{}^2\omega^2} \qquad (4)$$

$$G''_{LT} = G_{LT}\frac{\tau_{LT}\omega}{1+\tau_{LT}{}^2\omega^2} \qquad (5)$$

$$G_{LT} = QC[\eta]\frac{CRT}{M} \qquad (6)$$

$$\tau_{LT} = P\tau_{RZ} \qquad (7)$$

where Q and P are adjustable parameters. G' data in the lower ω region can be well fitted by addition of the LT term, while the difference in the calculated G'' with and without LT term are very small. Therefore, we first try to fit the G'' data and then further examine the fitting by addition of LT term.

Figure 4-4 shows the fitting results with eqs. (1)-(3) for data in Figure 2 by using three τ_{RZ}s therein. Note that, C, R, T and η_s are known ($G'' >> \omega\eta_s$) and $\alpha = 2$ for our solutions and we set p = 50 in eq (3) since the higher p only show very small difference at higher ω end. Thus, M can be treated as the single fitting parameter. The differences among three fitted lines using three τ_{RZ}s for G'' data and those for G' at higher ω are negligible when the M values are changed as designated in the Figure. The coincidence of the data and calculated lines for G'' is fine from terminal region to the lower ω portion of transition region. The calculated lines for both G' and G'' become slightly lower than the data at higher ω end. Since our purpose is to estimate the molecular weight of cellulose by fitting, but not to make fine fitting in the whole ω region, we ignore the small discrepancy.

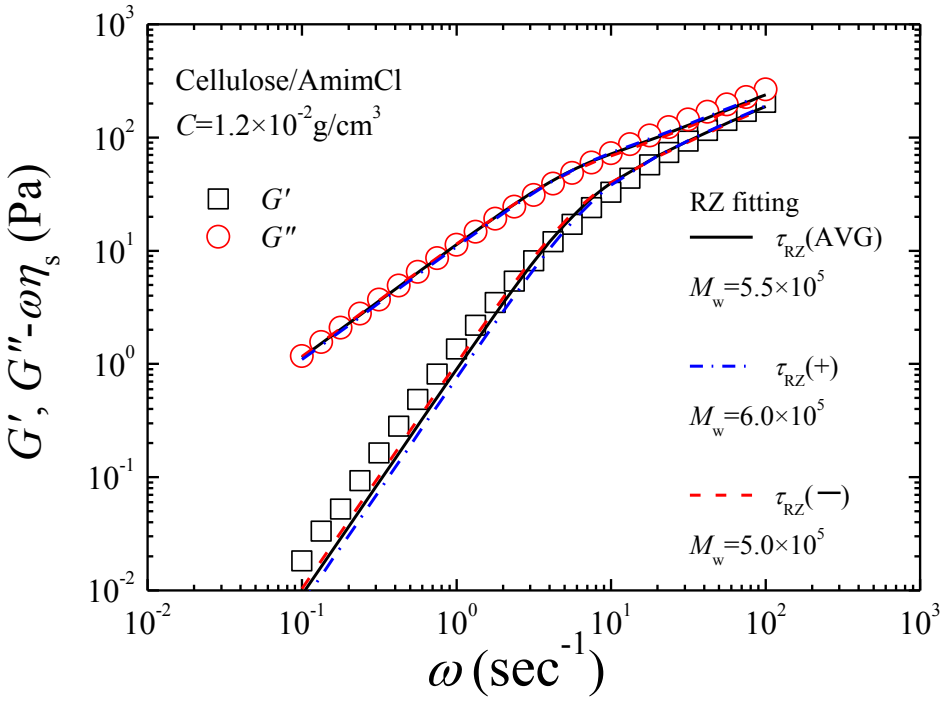

Figure 4-4. Double logarithmic plots of G' and G" vs ω for sample T1 with calculated values from RZ model by using different τ_{RZ} values in Figure 4-3 and adjusting M_w as designated in the figure. The symbols are also denoted in the figure.

Figures 4-5 and 4-6 show double logarithmic plots of G' and G'' vs ω for T1 and T2, respectively, together with calculated lines from eqs (1)-(3) with and without LT terms (eqs (4)-(7)). In the data analysis, first τ_{RZ} and its experimental error was determined as in Figure 4-3 and then the M values was estimated by fitting to eqs (4)-(6). The error of estimation for τ_{RZ} for T1 and T2 are around ±15%. Note that, τ_{RZ}(AVE) values obtained from above analysis coincided with the longest relaxation time of the Rouse model defined as $\tau_{RZ} = 6\eta^0 M/\pi^2 CRT$. The error of estimation for M, which correspond to weight-averaged molecular weight M_w, ΔM_w, are about ±10% in

these cases. Then by using thus obtained M_w and $[\eta]$ values obtained in Figure 1, LT terms are calculated. The best choice of P and Q in eqs (6) and (7) are 5 and 0.007, respectively, for T1 and T2 solutions in Figures 4-5 and 4-6. These values are the same as those reported by Inoue *et al.*[2), 3)] at $C[\eta] > 2.5$ for polystyrene in a good solvent.

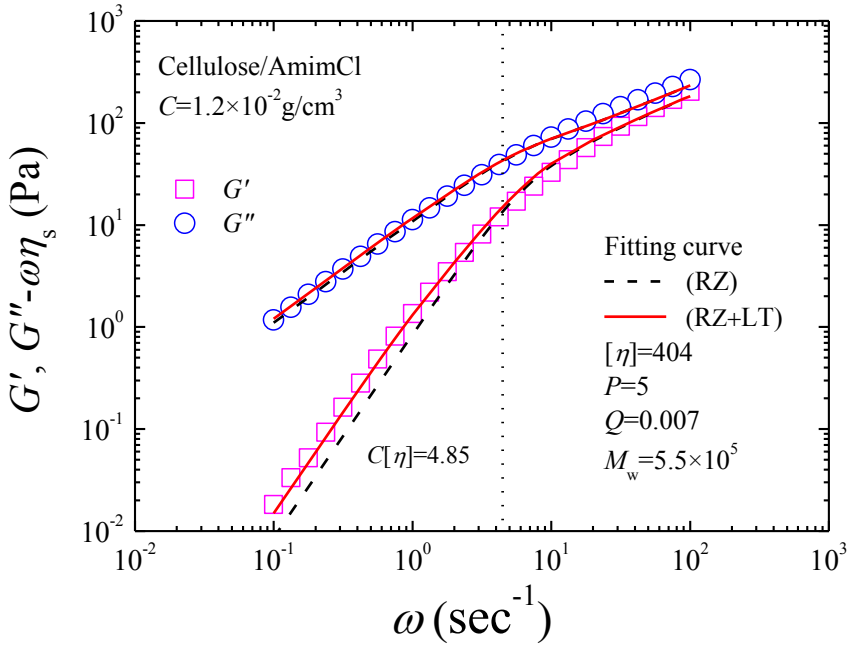

Figure 4-5. Comparisons of dynamic viscoelastic data for T1 solutions and RZ model with (broken lines) and without (solid lines) LT term. Symbols and parameters are denoted in the figure. Note that broken and solid lines for G" are almost superimposed.

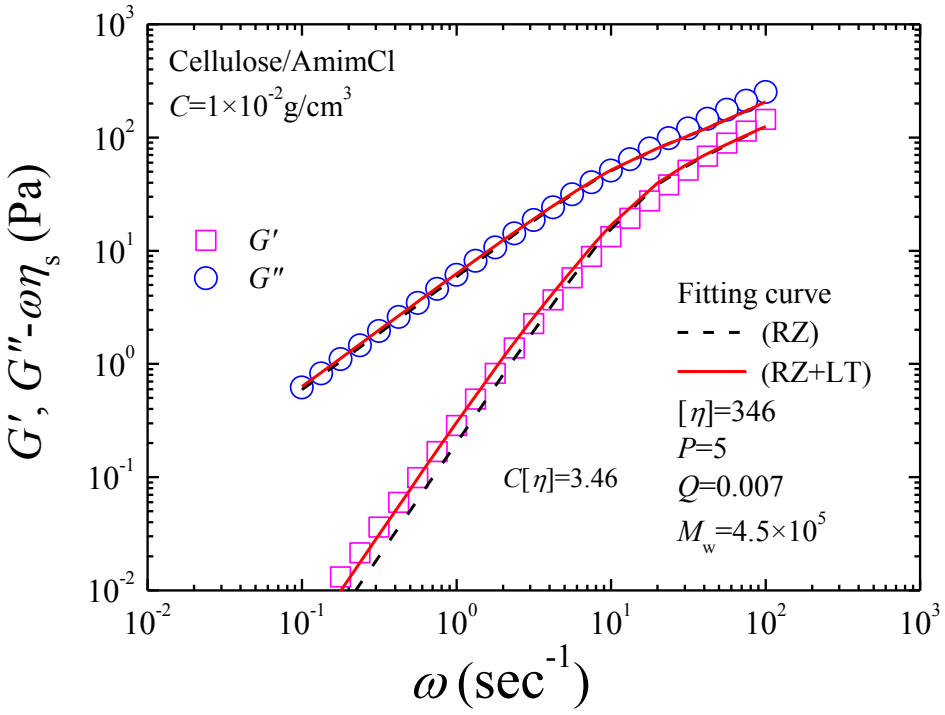

Figure 4-6. Comparisons of dynamic viscoelastic data for T2 solutions and RZ model with (broken lines) and without (solid lines) LT term. Experimentally determined τ_{RZ} was the same with calculated value from Rouse model (0.054 sec). Symbols and parameters are denoted in the figure.

We further tested the same procedure for T3 solution and diluted T1 solution. In these case, the longest relaxation time calculated from $\tau_{RZ} = 6\eta^0 M/\pi^2 CRT$ are slightly higher than τ_{RZ}(AVE) but coincided with τ_{RZ}(-). Better fitting results using τ_{RZ}(-) are obtained as shown in Figures 4-7 and 4-8. In these cases, the best choice of Q slightly changed to 0.009 but ΔM_w are also about ±10%.

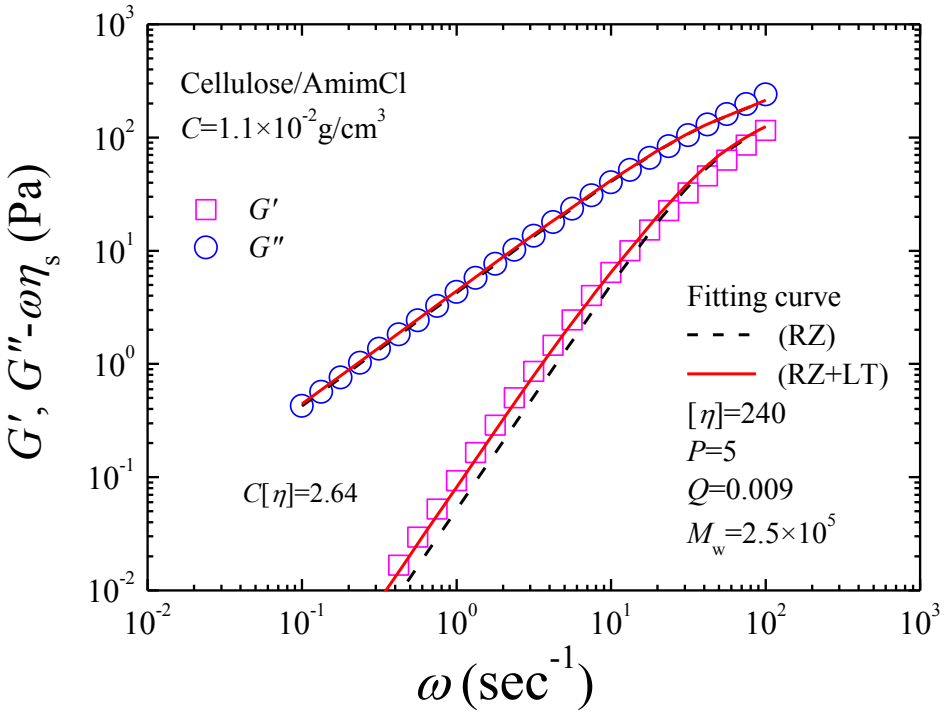

Figure 4-7. Comparisons of dynamic viscoelastic data for T3 solutions and RZ model with (broken lines) and without (solid lines) LT term. Experimentally determined τ_{RZ} was 0.0189 sec and the calculated value from Rouse model was 0.0201 sec. The latter is employed for the fitting. Symbols and other parameters are denoted in the figure.

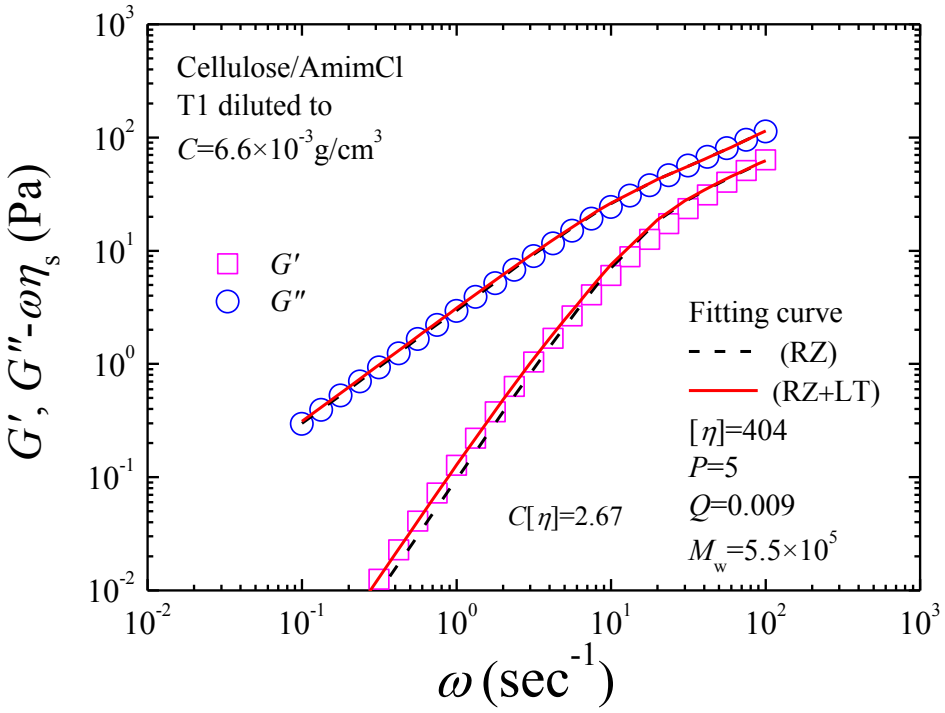

Figure 4-8. Comparisons of dynamic viscoelastic data for dilute T1 solutions and RZ model with (broken lines) and without (solid lines) LT term. Experimentally determined τ_{RZ} was 0.048 sec and the calculated value from Rouse model was 0.056 sec. The latter is employed for the fitting. Symbols and other parameters are denoted in the figure.

Comparing the results in Figures 4-6~4-8, we can point out that when RZ model is fitted to *G*" data by using M as a fitting parameter while fixing others, the calculated values of *G*" coincide with the experimental value up to lower ω end of transition region. It can be also pointed out that *G*' in the higher ω region (region on the right hand side of dotted line in Figure 4-5, the fitting curve for RZ and LT term are almost superimposed. The discrepancy between calculated and measured values in the

transition region is not so large. Therefore, by ignoring above small discrepancy we can estimate M_w of unknown samples as long as the parameters other than M is fixed and τ_{RZ} can be obtained with small error. LT term is useful to check the fairness of the fitting but we conclude that we can use this procedure to estimate M_w even for the case that $[\eta]$ is unknown, as long as τ_{RZ} can be obtained with relatively small error. Although the estimated M_w needed to be confirmed by different experiment, but it is useful to compare M_ws of different cellulose/IL solutions. More systematical examination of the procedure using well characterized pullulan samples will be reported elsewhere.

4.3 Summary

In summary, we conclude that measured G' and G'' can be well fitted with RZ model plus LT term in the terminal region but show small discrepancy in the transition region. In the so-called Rouse-like region, we can fix $\alpha = 2$ and use experimentally determined relaxation time as long as the relaxation time can be obtained with relatively small error. Consequently, molecular weight of the sample becomes single fitting parameter for RZ model. The fairness of the fitting can be further tested by addition of LT term. This fitting procedure can be used to estimate molecular weight of samples as long as the experimental error of relaxation time is small.

4.4 Referrence

1) Osaki K, Inoue T, Uematsu T, *Journal of Polymer Science: Part B: Polymer Physics Ed.*, **39**, 211-217 (2001)

2) Inoue T, Yamashita Y, Osaki K, *Macromolecules*, **35**, 9169-9175, (2002)

3) Osaki K, Inoue T, Uematsu T, Yamashita Y, *Journal of Polymer Science: Part B: Polymer Physics Ed.,* **40**, 1038–1045 (2002).

Chapter 5 Influence of the Bubble Burst to Chain Cessation of Cellulose during Dissolution Process into Ionic Liquids

5.1 Introduction

In previous Chapters, we examined dissolution conditions for different cellulose samples to obtain colorless uniform solutions, which means oxidation and thermal degradation are suppressed. We further examined chain cessation of samples, caused by bubble burst during dissolution, by comparing relative viscosity at the same concentration. Relative viscosity became higher for the solutions with more mild bubble burst speed. It is speculated that bubble burst causes sudden high stress in the solution, which result in chain cessation similar to the results reported by Keller[1)]. It was also speculated that the origin of bubbles are bound water of cellulose dissolved into ILs.

In this chapter, the effect of bubble-burst on the molecular weights of cellulose dissolved in ILs is discussed. The water content *WC* (*wt*%) of ILs are kept in a narrow range by the drying condition. The change of free water and bound water content in cellulose are briefly examined by changing the drying process as mentioned in Chapter 2. In this Chapter, change of *WC* during swelling and dissolution process are determined by Karl-Fischer titration to examine the effect of swelling. Then the difference in *M* of cellulose for solutions prepared by different conditions are

estimated by RZ fitting method examined in Chapter 4 and discussed with the change in *WC* and bubble bursting speed.

5.2 Experimental

Prescribed amounts of the dried cellulose samples and ILs are weighed and mixed into sample vials to prepare solutions at different concentrations. The mixtures are pre-heated at 0.1 atm, 80 °C for BmimCl and 60 °C for AmimCl, respectively, for a certain time to swell the samples. The samples are dissolved at 0.1 atm, 130°C for BmimCl and 100°C for AmimCl, for 4 hours and then the solutions are heated at 80°C, 0.1 atm until bubbles do not come out any more (about 48 hours). Finally, the samples are kept at 60°C and vials are occasionally tilted and/or rotated until concentration fluctuation cannot be observed by eyes.

To observe the swelling of samples during pre-heating, microscopic observation was carried out by a Keyence VHX-5900 as mentioned in Chapter 2. The water content *WC* of pre-heated mixtures and solutions are measured by Karl-Fischer titration method (KEM, MKC-501). *WC* after high temperature dissolution process was also determined by the titration method. Concentration *C* (g/cm^3) was converted from *c* (*wt*%) by using solution densities (see Chapter 2). Solvent viscosities are also corrected for the water content (see Chapter 2).

Dynamic viscoelastic measurements of cellulose solutions are carried out in an MCR-300 rheometer under N_2 atmosphere at 40 or 25 °C to cover the terminal region.

The strain amplitude was kept small (< 0.1) to ensure the linearity of the data.

5.3 Results and Discussions

During preheating process, swelling of cellulose fibers are observed. The swelling uniformly proceed in the early stage and then turn to irregular balloon-like structure after longer pre-heating time for low concentration samples (c < 2 *wt*%). At higher c, swelling become non-uniform due to partial integration of fibers. For samples with c < 2 *wt*%, the degree of swelling in early stage is examined by the diameter ratio, D/D_0, where D and D_0 is the diameters of swollen cellulose fibers and the initial dry fibers, respectively, measured at about 125 places of many fibers. As shown in Figure 5-1, observed diameters showed single peak distribution so that we obtained D_0 and D as simple averaged values. The time dependency of D/D_0 are shown in Figure 5-2. It can be seen that the values became constant for a certain time interval and then gradually tern to balloon-like structure reported previously.[2), 3)] When lower temperature are chosen for pre-heating, swelling goes slowly but become constant at the same D/D_0. When higher temperature is used. Fibers start to break up to small pieces as shown in Chapter 3. Note that, small bubbles come out mildly during the process, denoting slow evaporation of water.

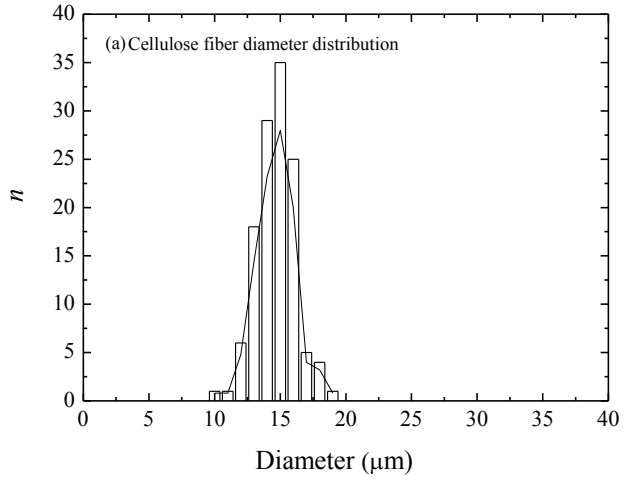

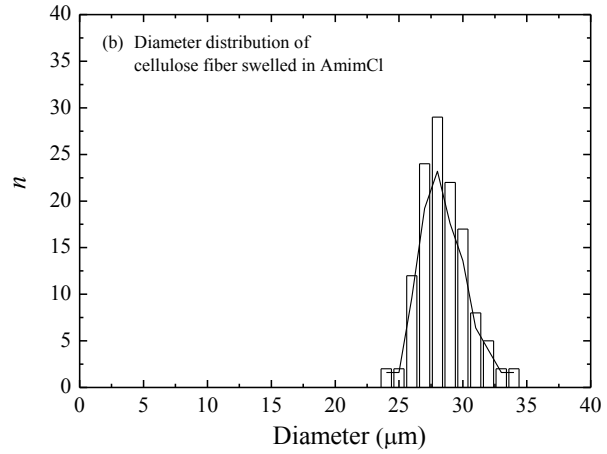

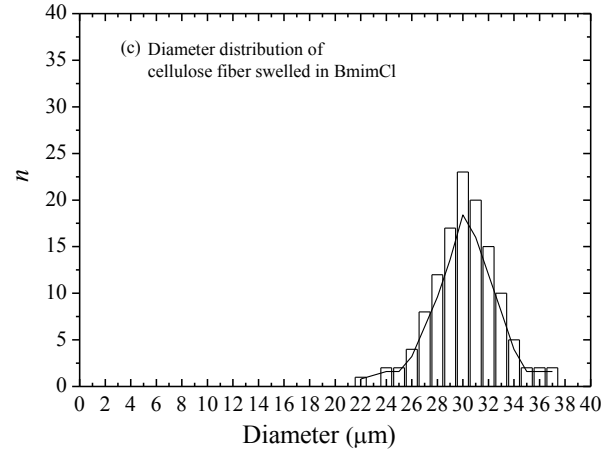

Figure 5-1. Diameter distribution of cotton fibers at different states (a) dried cellulose (b) swelled in BmimCl (0.5 *wt*%) and (c) swelled in AmimCl (0.5 *wt*%).

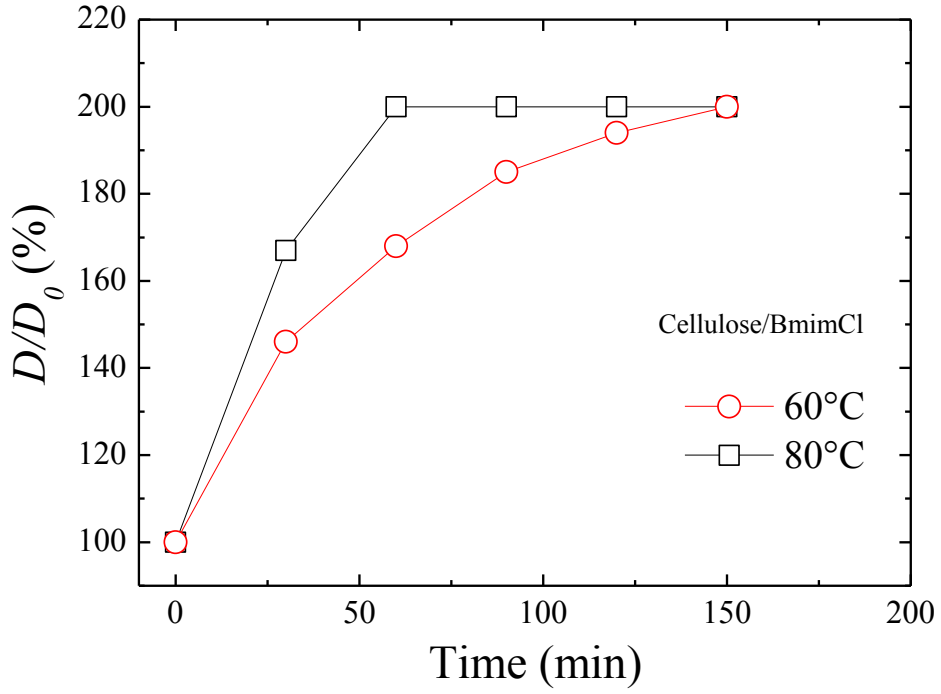

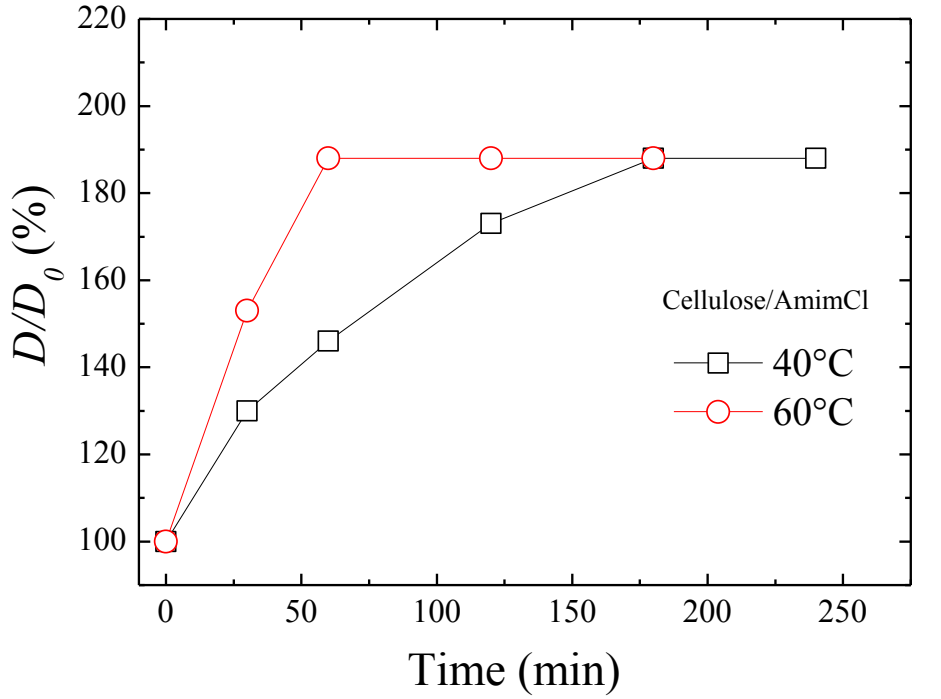

Figure 5-2. Time dependence of D/D_0 of cellulose in (a) BmimCl (0.5 *wt*%) and (b) AmimCl (0.5 *wt*%) with different preheat temperature at 0.1 atm.

Figure 5-3(a) shows time dependency of *WC* for cellulose/BmimCl and pure BmimCl. It is clear that *WC* increase with time even for BmimCl, denoting that the measured values are influenced by water adsorption during the measuring process. To estimate the amount of water dissolved from cellulose fiber, $\Delta WC = WC$(sample) – *WC*(BmimCl or AmimCl) are plotted against preheating time in Figure 5-3(b). It can be seen that the ΔWC at 45 - 75 min become roughly constant for each sample and the values tend to be higher for higher concentration samples. That is, water in cotton is dissolved into ILs while it is evaporated from ILs during the preheating process, resulting in certain stationary value depending on the amount of cellulose.

At later pre-heating process, when balloon-like swollen fibers increased, at the middle of dissolution process at high temperatures, and samples with higher concentrations ($c > 2$ *wt*%), *WC* cannot be measured since the collected liquid portion of samples turn gel-like when mixed with titration chemicals. However titration become possible again when dissolution was completed. Therefore, we set 1 hour pre-heating as the start point of dissolution of cotton/ILs mixture at higher temperature up to 2 *wt*% of cellulose to examine the effect of bubble burst on the molecular weight of dissolved cellulose.

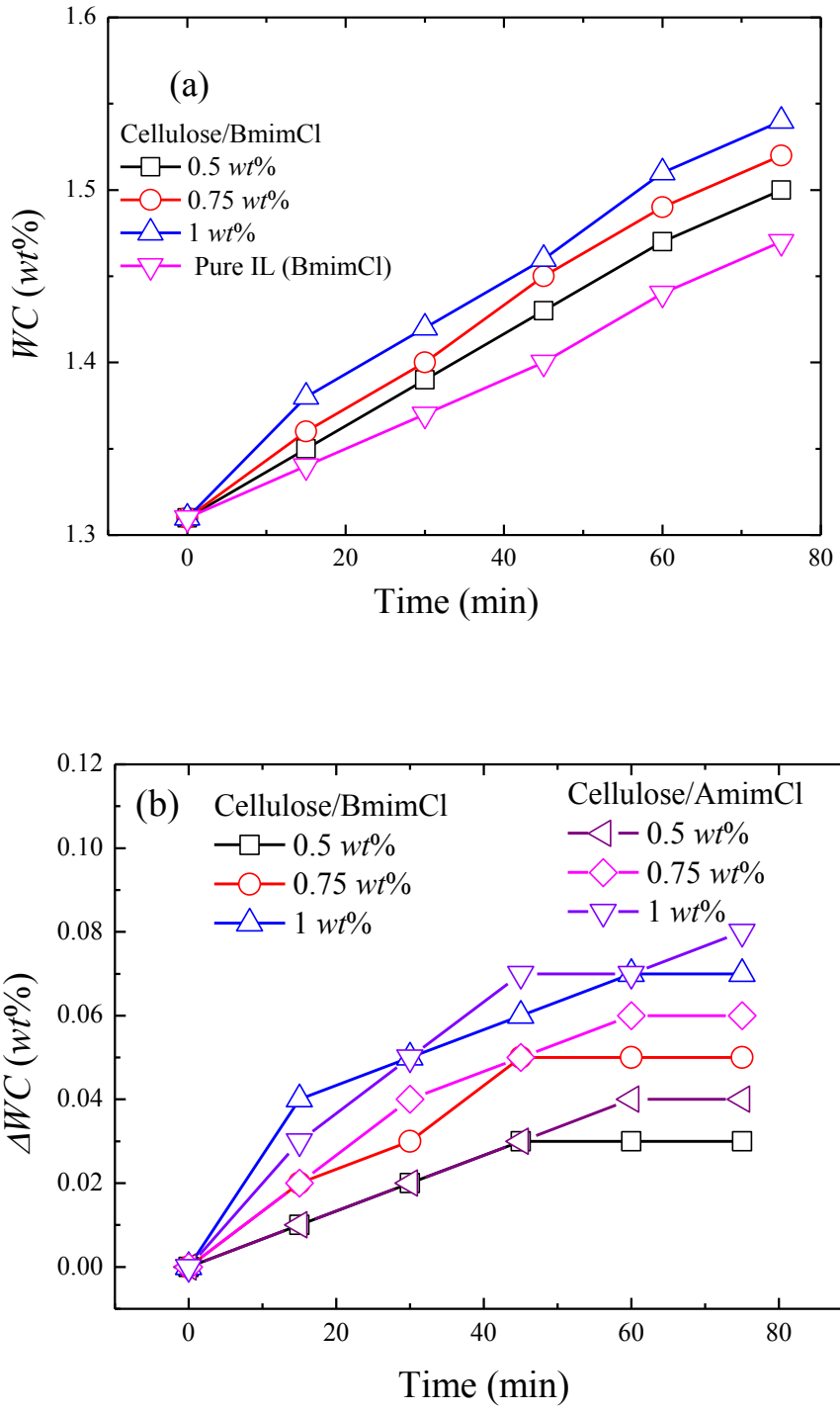

Figure 5-3. Water content time dependence of cellulose/ILs during the preheat treatment for a; cotton/BmimCl and b; the water content increment+Δ*WC* during the preheat treatment for cotton in BmimCl and AmimCl.

Figure 5-4 shows the representative *WC* data for (a) cotton/BmimCl and (b) cotton/AmimCl before pre-heating, after 1 hour pre-heating, after 15 minutes heating at higher temperatures, (130°C 0.1 atm for BmimCl and 100°C 0.1 atm for AmimCl), and at the end of high temperature dissolution. When high temperature heating was started, small bubbles began to come out continuously so that *WC* increased. During further heating, the bubbles came out and burst fiercely, then bubble burst gradually diminished as fibers disappeared. After 4 and 6 hours heating for BmimCl and AmimCl, respectively, there was no more bubbles observed by eyes. The *WC* values became even lower than the initial values, indicating that the bubbles are from the water in cellulose. The bubble burst was relatively mild in AmimCl mixture than in BmimCl mixture, probably due to the lower heating temperature and lower viscosity for AmimCl. The cotton/ILs solutions thus prepared are preserved in a heat oven till the concentration fluctuation disappear and then viscoelastic measurements are carried out.

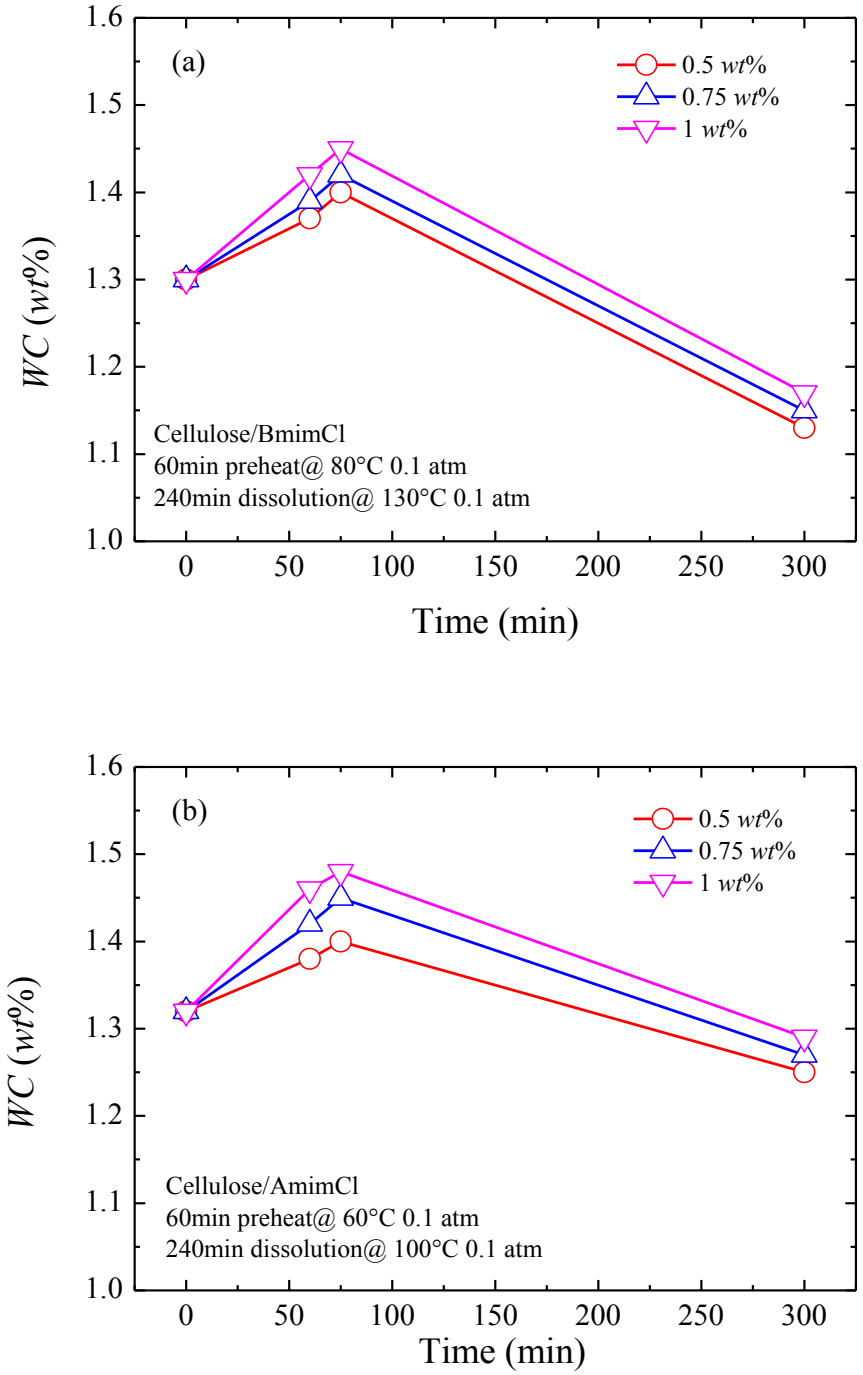

Figure 5-4. Time dependence of *WC* for cellulose/ILs during the dissolution process stated from the same initial WC but different *c* (*wt*%) for (a) cellulose /BmimCl and (b) cellulose /AmimCl. Sybomls are denoted in the figure.

By choosing appropriate measuring temperature, terminal region behavior and lower frequency part of transition region behavior was observed for dynamic viscoelastic data of all the solutions tested. In order to discuss the change in M_w, the data are fitted with Rouse-Zimm (RZ) model, in which G' and G" can be expressed by the following general formulae,

$$G''(\omega) = \frac{CRT}{M}\sum_{p=1}^{N}\frac{\omega\ \tau_P}{1+\omega^2{\tau_P}^2} + \omega\eta_s \qquad (1)$$

$$G'(\omega) = \frac{CRT}{M}\sum_{p=1}^{N}\frac{\omega^2{\tau_P}^2}{1+\omega^2{\tau_P}^2} \qquad (2)$$

$$\tau_p = \frac{\tau_{RZ}}{p^{\alpha}} \qquad (3)$$

where R is the gas constant, T is the temperature, ω is the frequency and η_s is solvent viscosity. τ_p is the relaxation time of p-th normal mode defined in eq.3 with τ_{RZ}. The parameter α denotes the hydrodynamic interaction strength; α = 2 corresponds to non-draining limit, while α = 1.5 corresponds to free-draining limit. In this study, we fix α = 2 and p = 50 for simplicity and use experimentally determined τ_{RZ} to use M as the only one fitting parameter.

The fitting is performed to well fit G" data since the correction term (long time term) is negligible for G", while it is not negligible for G' as discussed in the Chapter 4. As shown in the Chapter 4, G' become well fitted by including the correction term without changing fitting parameters in RZ model. Therefore, we assume that the fitted results are reliable as long as the longest relaxation time obtained phenomenologically and calculated by Rouse model, $\tau_{RZ} = 6\eta^0 M/\pi^2 CRT$, using fitted M coincide within a reasonable error.

Figure 5-5 shows examples of double logarithmic plots of G' and G'' vs ω for cotton/BmimCl solutions with fitted results. Note that τ_{RZ} phenomenologically determined from terminal region data and calculated by Rouse model coincide well for Figure 5-5(a). On the other hand, there was relatively large difference for the longest relaxation time by 2 methods. Therefore, we slightly tuned τ_{RZ} to obtain better fitting and coincidence of the longest relaxation time. By this treatment, M_w changed from 1.2×10^5 to 1.8×10^5 denoting that there exist larger error for estimated M_w in Figure 5-5(b). However, it is enough to say that the M_w is lower for Figure 5-5(b) than that for Figure 5-5(a).

The estimated M_w value seems to depend on the *WC* after pre-heating as shown in Figure 5-5. To check this point, we further examined the trend of change in M_w by adding small amount of water after pre-heating for cotton/AmimCl solutions. Figure 5-6 show double logarithmic plots of G' and G'' vs ω for cotton/AmimCl solutions thus prepared with fitted results. The sample with higher *WC* tend to result in the lower M_w. Together with the results in Figure 5-2 that *WC* after pre-heat increase with the amount of cellulose, we further tested for different concentrations. The representative examples are shown in Figure 5-7. Hereafter, when the coincidence of two relaxation time is not so good, τ_{RZ} was slightly tuned to obtain better results as employed in Figure 5-5(b). A few more experiments prepared under different conditions are shown in Figure 5-8~5-10.

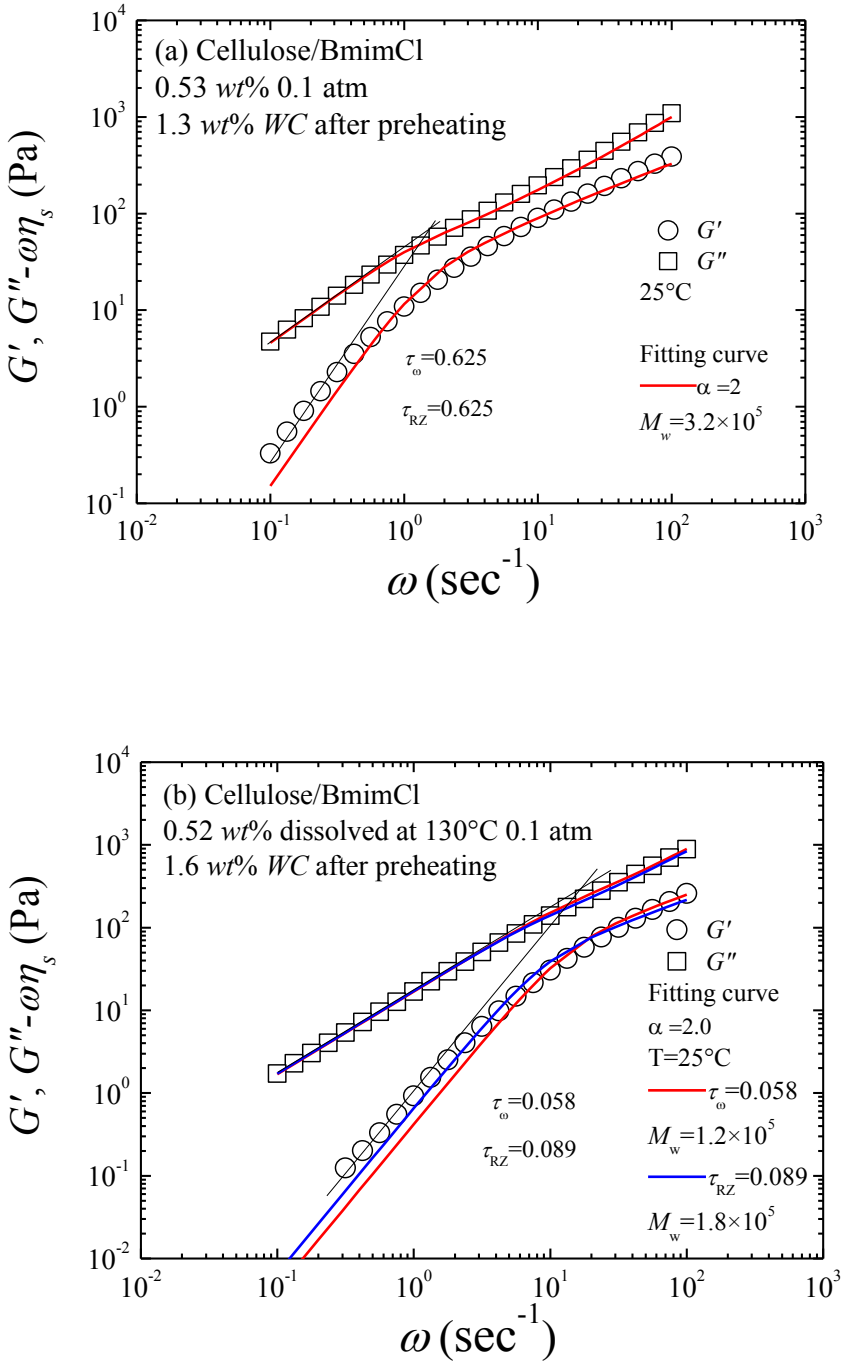

Figure 5-5. Double logarithmic plots of *G*' and *G*" vs ω for cellulose/BmimCl prepared at 130 °C 0.1 atm with different initial *WC* (a) 1.3 wt% after pre-heating and (b) 1.6 wt% after pre-heating. Lines going through the data are fitted lines by RZ model. The symbols are denoted in the figure.

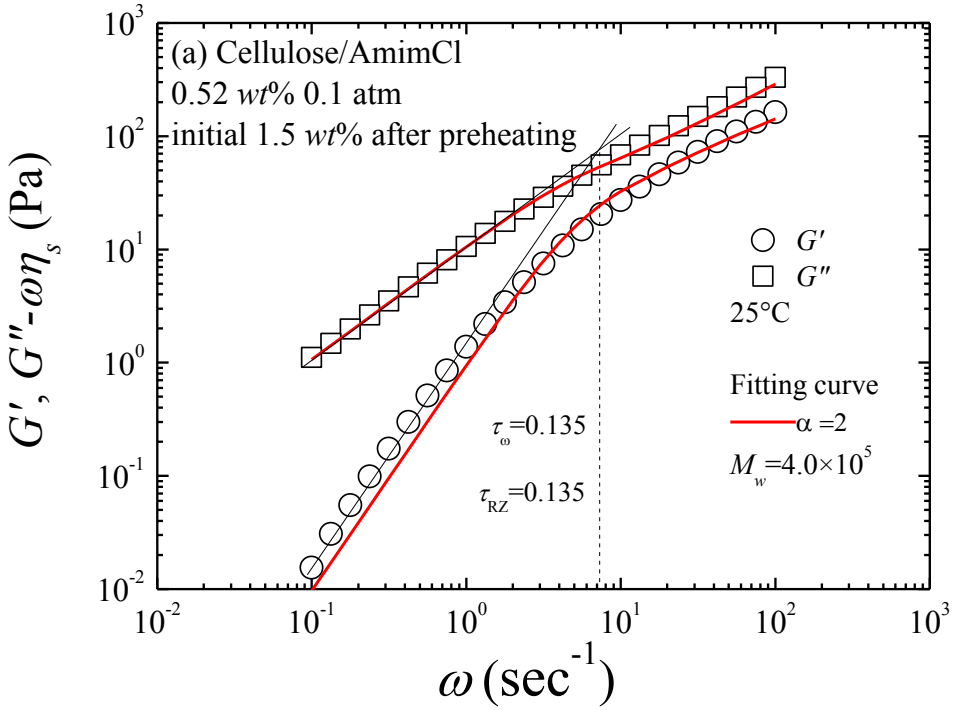

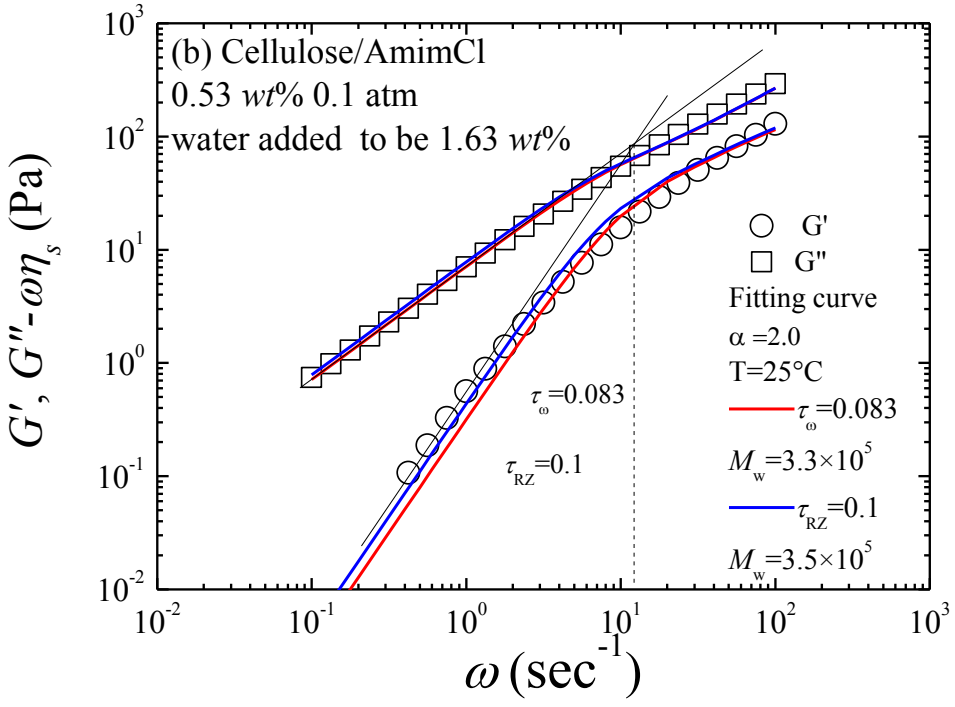

Continued to the next page

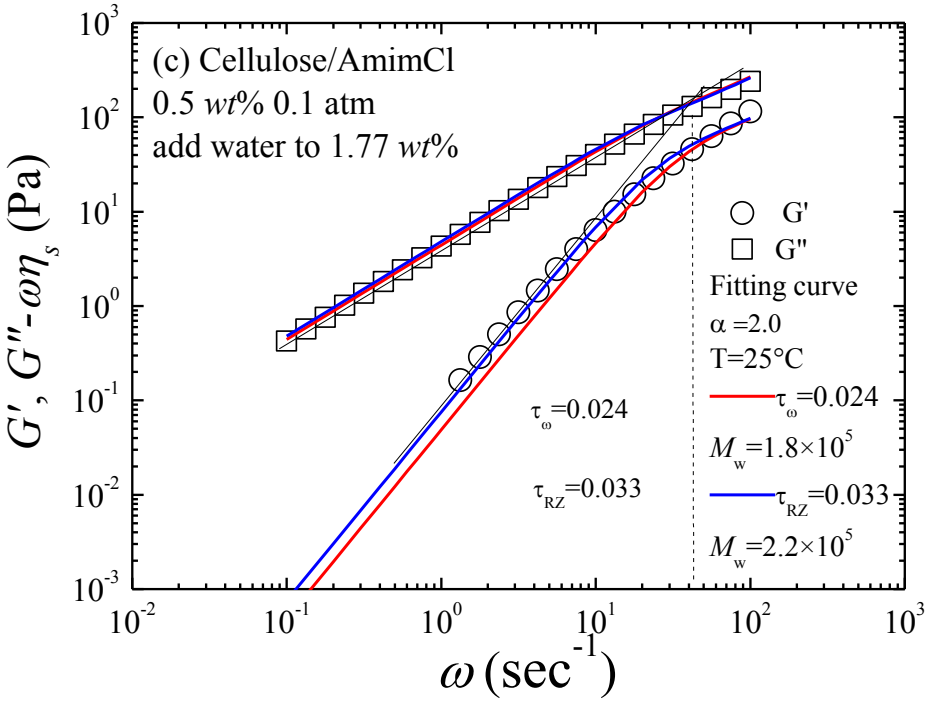

Figure 5-6. Double logarithmic plots of *G*' and *G*" vs ω for cellulose/AmimCl prepared at 100 °C 0.1 atm with the same *c* (0.5 *wt*%) but with different water content (a) 1.5 *wt*%; (b) 1.63 *wt*%; (c) 1.77 *wt*%. The symbols are denoted in the figure.

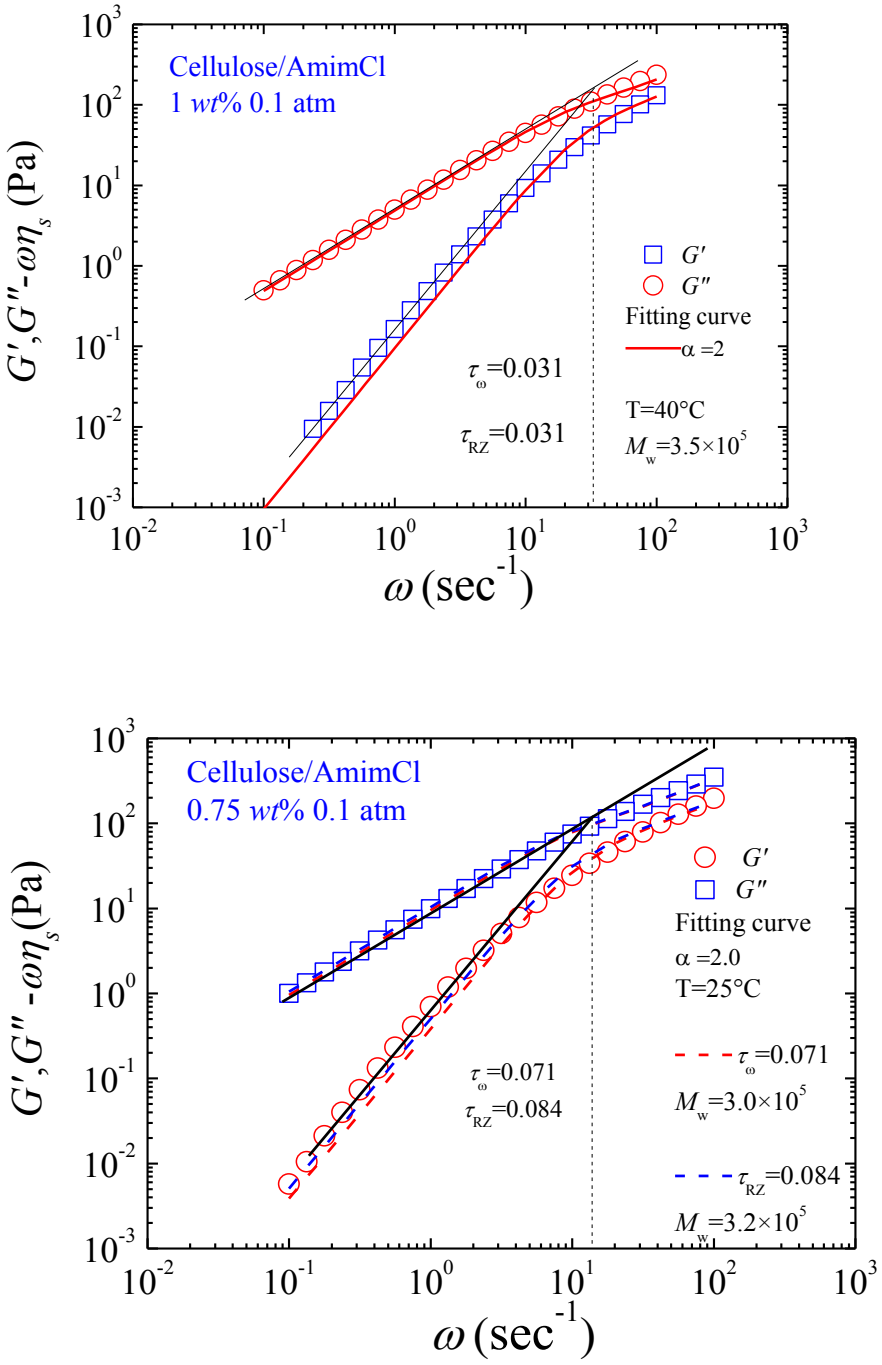

Figure 5-7. Double logarithmic plots of *G*' and *G*" vs ω for cellulose/AmimCl prepared at 100 °C 0.1 atm for (a) *c*=1 *wt*% and (b)*c*=0.75 *wt*%. The symbols are denoted in the figure.

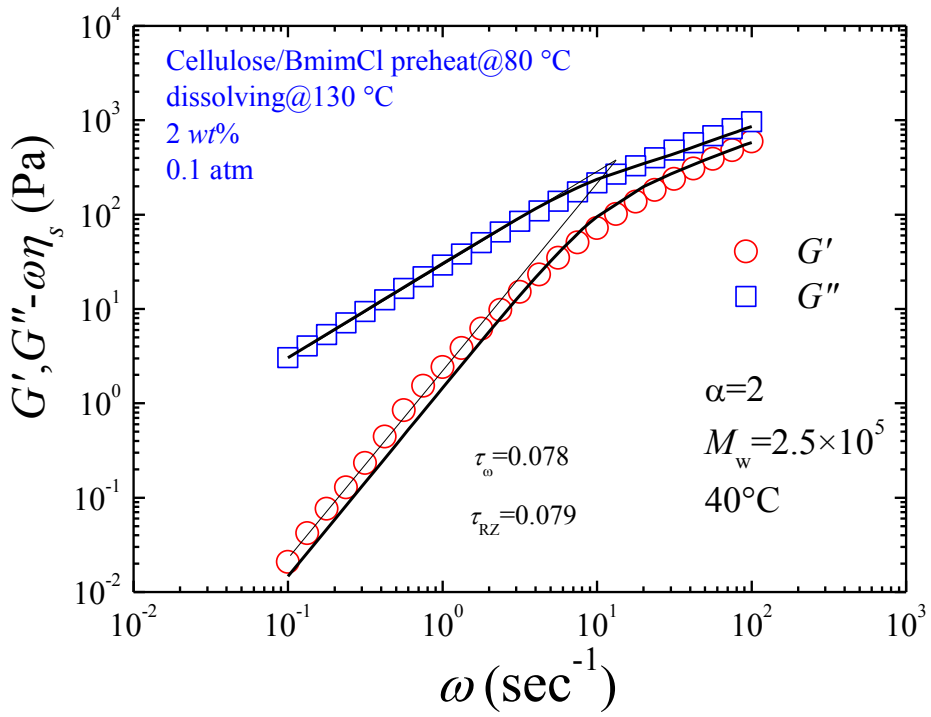

Figure 5-8. Double logarithmic plots of G' and G" vs ω for cotton/AmimCl prepared at 130 °C 0.1 atm c=2 wt% fitting by RZ model. The symbols are denoted in the figure. Note that τ_{RZ} obtained with two methods are coincided.

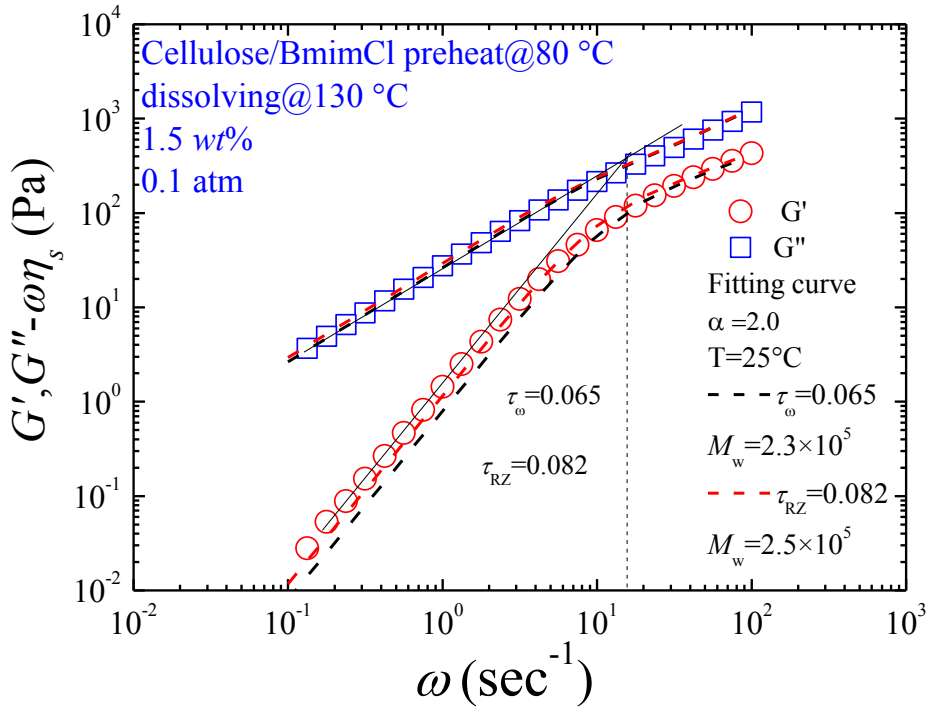

Figure 5-9. Double logarithmic plots of G' and G" vs ω for cotton/AmimCl prepared at 130 °C 0.1 atm c=1.5 wt% good fitting with RZ model was obtained from τ_{RZ} obtained by RZ calculation. The symbols are denoted in the figure.

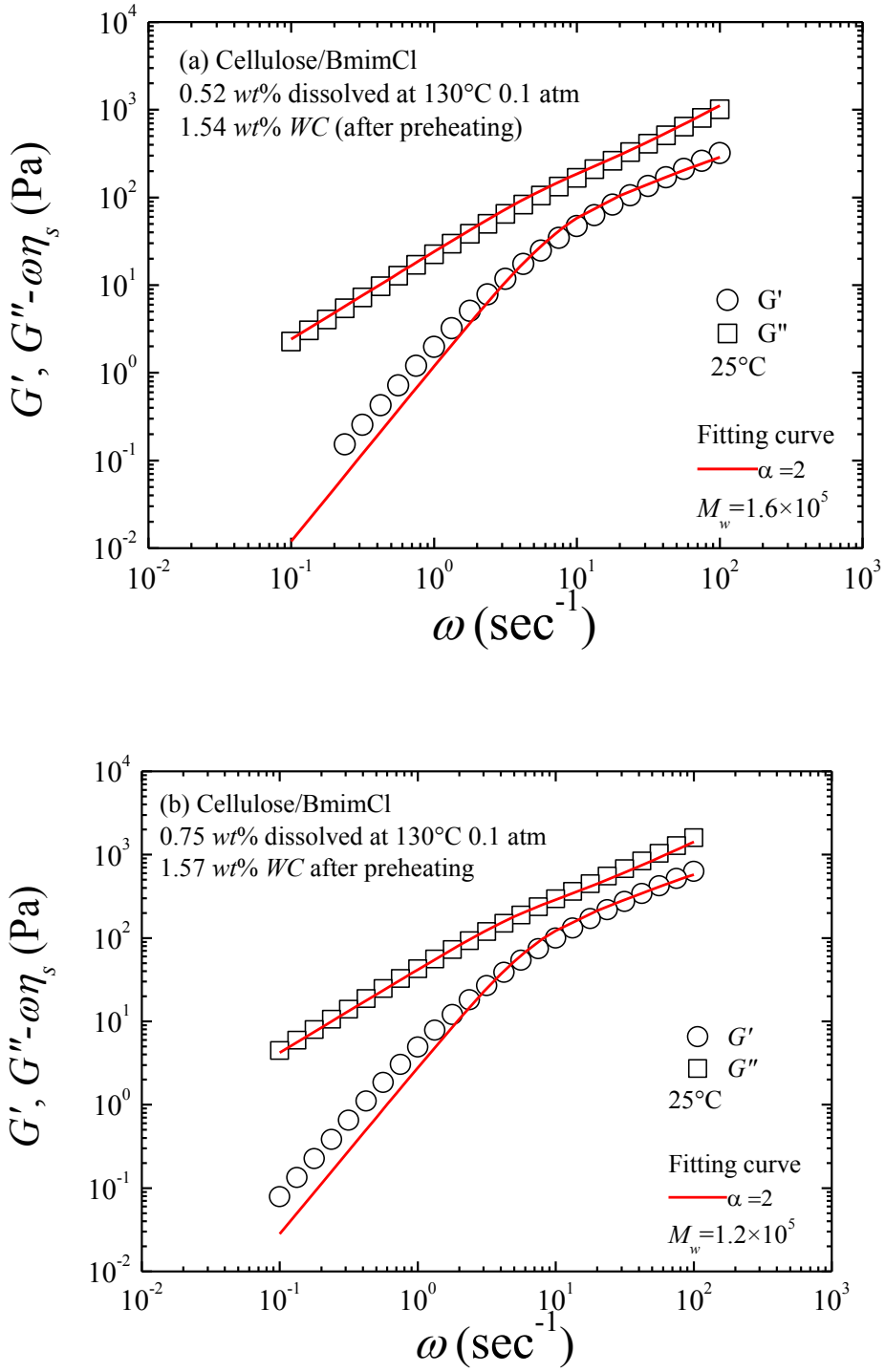

Figure 5-10. Double logarithmic plots of *G*' and *G*" vs ω for cotton/BmimCl prepared at 130 °C 0.1 atm at different concentration (a) 0.5 *wt*%; (b) 0.75 *wt*% fitting by RZ model. τ_{RZ} was the calculated value from Rouse model employed for the fitting. The symbols are denoted in the figure.

Figures 5-11 and 5-12 summarize the molecular weight estimated for all the solutions. Close symbols denote the data obtained for solutions in which the longest relaxation times by two methods are coincided, while open symbols are cases that they differ more than 15%. In the latter case, τ_{RZ} is slightly tuned to get better results. Therefore, the latter have larger error than former but we can still use them to discuss the relation between *WC* after pre-heat and M_w. It is clear that close symbols are roughly constant for each ILs denoting that correlation between *WC* after pre-heat and M_w is poor. As seen in these figures reproducibility of M_w is poor for each concentrations. It can be also pointed out that the M_w in AmimCl tend to be somewhat larger than in BmimCl, which may imply that bubble burst and resulting chain cessation is mild for AmimCl.

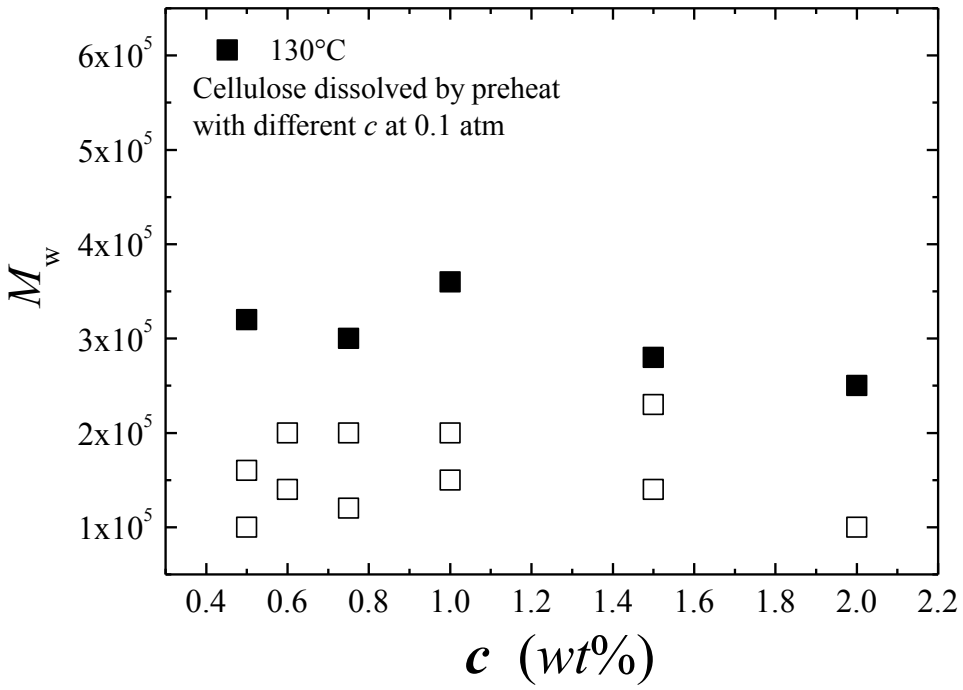

Figure 5-11. Estimated M_w of cellulose dissolved in BmimCl prepared at different concentrations. Filled symbols denote the data for higher reliability as describe in the text (good agreement of two estimations of the longest relaxation time. Open symbols denote the data obtained by slightly tuning the longest relaxation time as explained in the text.

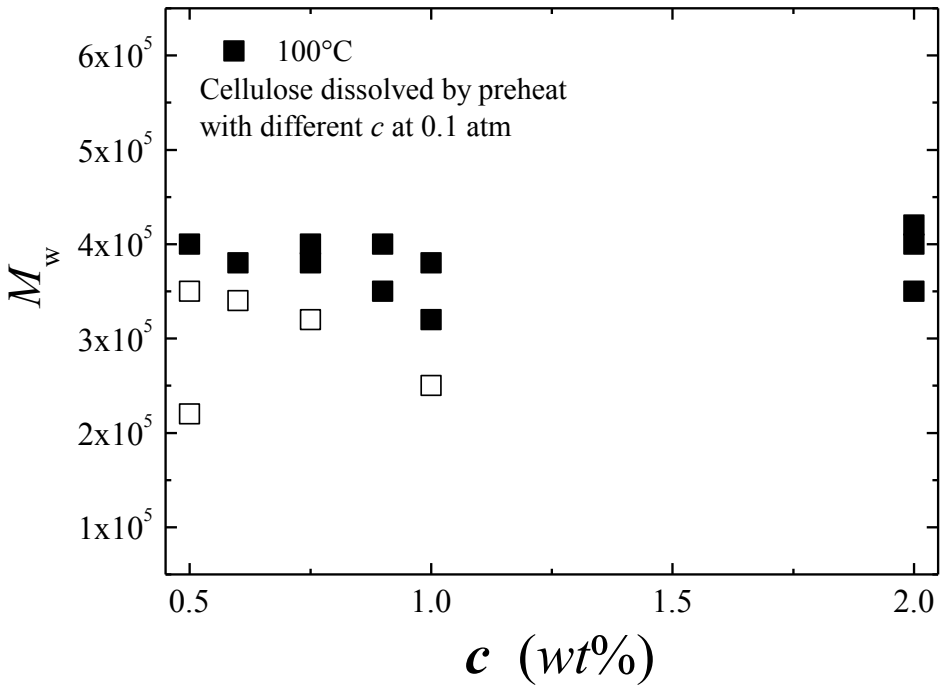

Figure 5-12. Estimated M_w of cellulose dissolved in BmimCl prepared at different concentrations. Filled symbols denote the data for higher reliability as describe in the text (good agreement of two estimations of the longest relaxation time. Open symbols denote the data obtained by slightly tuning the longest relaxation time as explained in the text.

As reported in Chapter 3, cellulose can be fully dissolved in AmimCl over a wide temperature range with preheating treatment. Further dissolution experiments are carried out to investigate the difference of cellulose/AmimCl solutions at different temperature under 0.1 atm. The results are summarized in Figure 10. All the cellulose/AmimCl solutions are prepared with fixed concentration 2 *wt*%. The dissolution time of cellulose at higher temperatures is shorter than lower temperatures.

For the samples dissolved at 80 and 90 °C about 2 days continuous heating is needed. It can be seen that with the increasing of dissolving temperature the M_w got decreased gradually. It can be speculated that by controlling the dissolution temperature, the bubble-burst speed can be controlled. With this dissolution method the M_w of cellulose in AmimCl can be controlled on a certain extent under 0.1 atm with different temperature.

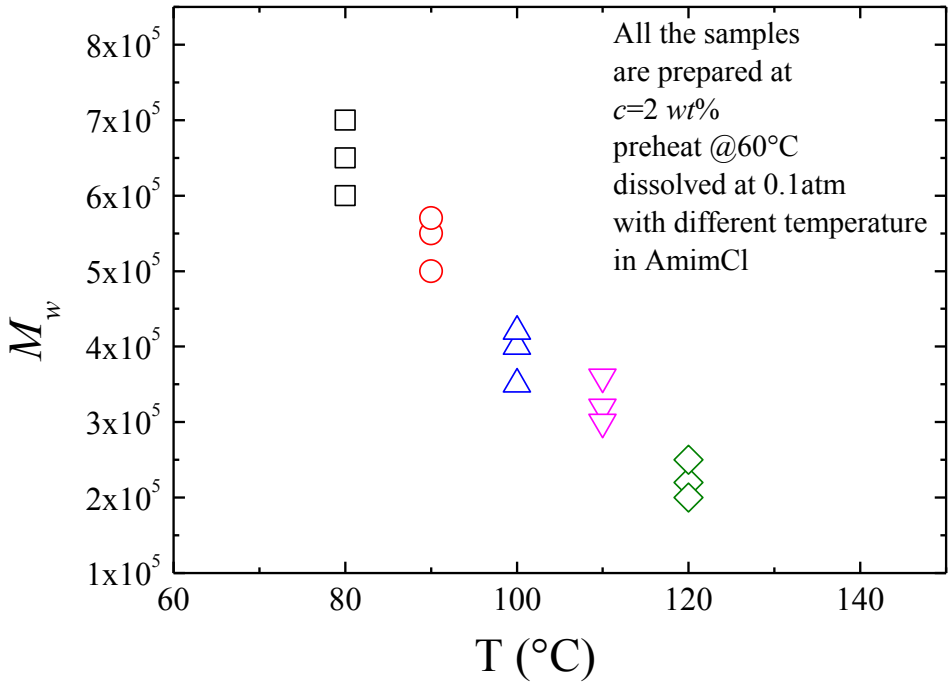

Figure 5-13. Estimated M_w of cellulose dissolved in AmimCl with different dissolving temperature at 0.1 atm.

5.4. Conclusion

We examined the change in water content (*WC*) of cellulose/ILs during the preheat treatment and found that *WC* became almost constant for later stage of the treatment, which increased with amount of cellulose. To investigate the influence of initial *WC*, different water content samples are examined and found that the correlation between initial *WC* and resulting M_w of cellulose is poor. Moreover, reproducibility of M_w is poor for each concentrations. However, M_w of cellulose in AmimCl can be controlled on a certain extent under 0.1 atm with different dissolving temperature. It is concluded that controlling the bubble-burst speed is essential factor for the M_w of cellulose dissolved in ILs solution.

5.5Reference:

1) Keller A and Odell JA. *Colloid Polym. Sci*., **263**,181 (1985).

2) Tripp VW, Rollins ML *Anal.Chem*., **24**, 1721 (1952).

3) Cuissinat C, Navard P, *Macromol.Symp*., **244**, 1 (2006).

Chapter 6. Conclusions

In this thesis, viscoelastic properties of cellulose from different origins in BmimCl, AmimCl, and EmimAc are studied in comparison with the behaviors of standard Pullulan in ILs dilute solutions.

In chapter 3, dissolution conditions of avicel, cotton, nadelholz sulfur pulp (NSP), and linter pulp into 1-butyl-3-methylimidazolium chloride (BmimCl), 1-allyl-3-methylimidazolium chloride (AmimCl) and 1-ethyl-3-methylimidazolium acetate (EmimAc) are examined to obtain less damaged (less colored and higher viscosity) uniform solutions. The tested dissolution conditions are inadequate for EmimAc. To suppress degradation of cellulose, depressed conditions without mechanical stirring are effective for BmimCl and AmimCl systems. Under those conditions, cotton and NSP can be dissolved uniformly with less change in the color but avicel and linter cannot be. When the bubble burst was suppressed by pre-heating, color change of solution was more suppressed. The pre-heated cotton solution showed higher relative viscosity than others.

In chapter 4, the zero shear viscosities of cellulose/AmimCl solutions and solvents are obtained by using oscillatory and steady shear flow measurements. The intrinsic viscosity of cellulose in AmimCl are determined by the extrapolate method. The dynamic viscoelastic properties of cellulose ILs solutions can be well fitted with RZ model plus LT term in the terminal region but show small discrepancy in the transition region. In the so-called Rouse-like region, we can fix $\alpha = 2$ and use experimentally determined relaxation time as long as the relaxation time can be obtained with relatively small error within ±15% . Consequently, molecular weight of the sample becomes single fitting parameter for RZ model. The fairness of the fitting can be

further tested by addition of LT term. This fitting procedure can be used to estimate molecular weight of samples as long as the experimental error of relaxation time is small.

In chapter 5, the change in water content (*WC*) of cellulose/ILs during the preheat treatment were examined and it was found that *WC* became almost constant for later stage of the treatment, which increased with amount of cellulose. To investigate the influence of initial *WC*, different water content samples are examined and found that the correlation between initial *WC* and resulting M_w of cellulose is poor. Moreover, reproducibility of M_w is poor for each concentrations. However, M_w of cellulose in AmimCl can be controlled on a certain extent under 0.1 atm with different dissolving temperature. Controlling the bubble-burst speed is essential factor for the M_w of cellulose dissolved in ILs solution.

Publications

1. Study on the Dissolution Process of Different Kinds of cellulose into Ionic Liquids

   Zhe Xu, Yoshiaki Takahashi

   Nihon Reoroji Gakkaishi (Journal of the Society of Rheology, Japan) accepted for publication.

2. Molecular Weight Estimation of Cellulose in Ionic liquid Solution by Fitting Dynamic Viscoelastic Data to Rouse Model.

   Zhe Xu, Yoshiaki Takahashi

   Nihon Reoroji Gakkaishi (Journal of the Society of Rheology, Japan) accepted for publication.

3. Influence of the Bubble Burst to Chain Cessation of Cellulose during Dissolution Process into Ionic Liquids

   Zhe Xu, Yoshiaki Takahashi Submitted

Acknowledgment

Firstly, I would like to express my sincere gratitude to my advisor **Associate Prof. Yoshiaki Takahashi** for the continuous support of my Ph.D study and related research for his patience, motivation, and immense knowledge. Under his guidance I have learnt a lot of new frontier analysis methods and obtained a lot of new ideas from the crossing fields to widen my research from various perspectives. All of these will be very important for my career in future. I could not have imagined having a better advisor and mentor for my six years study in Kyushu University.

Besides my advisor, I would like to thank **Assistant Prof. Akihiko Takada** for their insightful comments and encouragement throughout the six years. My sincere thanks also go to Dr. **Hiroya Nishikawa**, who gave me some new knowledge. Without their precious support it would not be possible to conduct this research.

I also thank my fellow lab mates in for the stimulating discussions, for the sleepless nights we were working together before deadlines, and for all the fun we have had in the last six years.

Last but not the least, I would like to thank my family: my parents and wife for supporting me spiritually and financially throughout writing this thesis and my life in general.